15. Saisho Y, Butler AE, Manesso E, Galasso R, Zhang L, Gurlo T, Toffolo GM, Cobelli C, Kavanagh K, Wagner JD, Butler PC. Relationship between fractional pancreatic beta cell area and fasting plasma glucose concentration in monkeys. Diabetologia 2010; 53: 111–114.
16. Bassi C, Dervenis C, Butturini G, Fingerhut A, Yeo C, Izbicki J, Neoptolemos J, Sarr M, Traverso W, Buchler M. Postoperative pancreatic fistula: an international study group (ISGPF) definition. Surgery 2005; 138: 8–13.
17. Dindo D, Demartines N, Clavien P-A. Classification of Surgical Complications. Ann Surg 2004; 240: 205–213.
18. Holman RR, Paul SK, Bethel MA, Matthews DR, Neil HA. 10-year follow-up of intensive glucose control in type 2 diabetes. N Engl J Med 2008; 359: 1577–1589.
19. Kawamori R, Tajima N, Iwamoto Y, Kashiwagi A, Shimamoto K, Kaku K. Voglibose for prevention of type 2 diabetes mellitus: a randomised, double-blind trial in Japanese individuals with impaired glucose tolerance. Lancet 2009; 373: 1607–1614.
20. Standards of medical care in diabetes—2012. Diabetes Care 2012; 35 Suppl 1: S11–63.
21. Hutchins RR, Hart RS, Pacifico M, Bradley NJ, Williamson RC. Long-term results of distal pancreatectomy for chronic pancreatitis in 90 patients. Ann Surg 2002; 236: 612–618.
22. Ritzel RA, Butler AE, Rizza RA, Veldhuis JD, Butler PC. Relationship between beta-cell mass and fasting blood glucose concentration in humans. Diabetes Care 2006; 29: 717–718.
23. Nakamura Y, Higuchi S, Maruyama K. Pancreatic volume associated with endocrine and exocrine function of the pancreas among Japanese alcoholics. Pancreatology 2005; 5: 422–431.
24. Matsumoto I, Sawada T, Nakano M, Sakai T, Liu B, Ansite JD, Zhang HJ, Kandaswamy R, Sutherland DE, Hering BJ. Improvement in islet yield from obese donors for human islet transplants. Transplantation 2004; 78: 880–885.
25. Ishikawa O, Ohigashi H, Eguchi H, Yokoyama S, Yamada T, Takachi K, Miyashiro I, Murata K, Doki Y, Sasaki Y, Imaoka S. Long-term follow-up of glucose tolerance function after pancreaticoduodenectomy: comparison between pancreaticogastrostomy and pancreaticojejunostomy. Surgery 2004; 136: 617–623.
26. Murakami Y, Uemura K, Hayashidani Y, Sudo T, Hashimoto Y, Ohge H, Sueda T. Long-term pancreatic endocrine function following pancreatoduodenectomy with pancreaticogastrostomy. J Surg Oncol 2008; 97: 519–522.
27. Litwin J, Dobrowolski S, Orlowska-Kunikowska E, Sledzinski Z. Changes in glucose metabolism after Kausch–Whipple pancreatectomy in pancreatic cancer and chronic pancreatitis patients. Pancreas 2008; 36: 26–30.
28. Permert J, Ihse I, Jorfeldt L, von Schenck H, Arnquist HJ, Larsson J. Improved glucose metabolism after subtotal pancreatectomy for pancreatic cancer. Br J Surg 1993; 80: 1047–1050.
29. Katsumichi I, Pour PM. Diabetes mellitus in pancreatic cancer: is it a causal relationship? Am J Surg 2007; 194: S71–75.
30. Saruc M, Pour PM. Diabetes and its relationship to pancreatic carcinoma. Pancreas 2003; 26: 381–387.

Radiotherapy and Oncology 103 (2012) 25–31

Contents lists available at SciVerse ScienceDirect

Radiotherapy and Oncology

journal homepage: www.thegreenjournal.com

Proton RT in pancreatic cancer

A phase I/II study of gemcitabine-concurrent proton radiotherapy for locally advanced pancreatic cancer without distant metastasis ☆

Kazuki Terashima [a,*], Yusuke Demizu [a], Naoki Hashimoto [a], Dongcun Jin [a], Masayuki Mima [a], Osamu Fujii [a], Yasue Niwa [a], Kento Takatori [b], Naoto Kitajima [b], Sachiyo Sirakawa [c], Ku Yonson [c], Yoshio Hishikawa [a], Mitsuyuki Abe [a], Ryohei Sasaki [d], Kazuro Sugimura [e], Masao Murakami [a]

[a] Department of Radiology, Hyogo Ion Beam Medical Center; [b] Department of Internal Medicine, Kasai City Hospital; [c] Division of Hepato-Biliary-Pancreatic Surgery, Kobe University Graduate School of Medicine; [d] Division of Radiation Oncology, Kobe University Graduate School of Medicine; [e] Division of Radiology, Kobe University Graduate School of Medicine, Hyogo, Japan

ARTICLE INFO

Article history:
Received 20 August 2011
Received in revised form 15 December 2011
Accepted 20 December 2011
Available online 31 January 2012

Keywords:
Proton radiotherapy
Gemcitabine
Pancreatic cancer
Locally advanced
Chemoradiotherapy

ABSTRACT

Purpose: We conducted the study to assess the feasibility and efficacy of gemcitabine-concurrent proton radiotherapy (GPT) for locally advanced pancreatic cancer (LAPC).
Materials and methods: Of all 50 patients who participated in the study, 5 patients with gastrointestinal (GI)-adjacent LAPC were enrolled in P-1 (50 Gy equivalent [GyE] in 25 fractions) and 5 patients with non-GI-adjacent LAPC in P-2 (70.2 GyE in 26 fractions), and 40 patients with LAPC regardless of GI-adjacency in P-3 (67.5 GyE in 25 fractions using the field-within-a-field technique). In every protocol, gemcitabine (800 mg/m^2/week for 3 weeks) was administered concurrently. Every patient received adjuvant chemotherapy including gemcitabine after GPT within the tolerable limit.
Results: The median follow-up period was 12.5 months. The scheduled GPT was feasible for all except 6 patients (12%) due to acute hematologic or GI toxicities. Grade 3 or greater late gastric ulcer and hemorrhage were seen in 5 patients (10%) in P-2 and P-3. The one-year freedom from local-progression, progression-free, and overall survival rates were 81.7%, 64.3%, and 76.8%, respectively.
Conclusion: GPT was feasible and showed high efficacy. Although the number of patients and the follow-up periods are insufficient, the clinical results seem very encouraging.
 Radiotherapy and Oncology 103 (2012) 25–31

The prognosis of pancreatic cancer is poor, with a five-year survival rate of about 5% in total [2]. Only radical surgical resection has been shown to cure the condition, although the five-year survival rate remains low at about 10–20%. And only 15–20% of all patients with pancreatic cancer can be treated by resection, while the other patients cannot undergo resection because of local invasion or distant metastasis at diagnosis [4,9].

For the treatment of non-resectable pancreatic cancers, chemoradiotherapy (CRT) with concurrent 5-fluorouracil (5-FU) is historically considered the standard therapy for locally advanced pancreatic cancer (LAPC) [6,18,26]. Recently, based on a background of favorable results of gemcitabine-based chemotherapy [1,9], and the fact that gemcitabine is a potent radio-sensitizer [16], many studies on gemcitabine-concurrent CRT have been performed for LAPC [7,17,20,24], and indicate the possibility of an improvement in survival. These studies have shown that reduction of the irradiation doses and target fields was necessary when gemcitabine was administered at or near the full dose (1000 mg/m^2). In contrast, a reduction of the gemcitabine dose was needed when irradiation was administered at doses over 50 Gy, which is necessary for the local control of malignant tumors. The reason for these restrictions of the chemoradiotherapy was speculation that the region of gastrointestinal (GI) tract located near the pancreas was irradiated beyond tolerable doses. Consequently, we thought that proton beam radiotherapy could deliver higher dose above 50 Gy concurrently with a higher dose of gemcitabine to a larger field containing the draining and paraaortic lymph nodes and peripheral regions surrounding the celiac artery and superior mesenteric artery.

Radiotherapy using protons or carbon-ions is currently attracting worldwide interest because of its physical properties including superior dose distribution to a target, which allows selective irradiation to the tumor, while minimizing irradiation of the surrounding normal tissues [10,15,25]. In our pilot study, proton beam radiotherapy alone was performed at doses of 40 and 50 GyE for patients with LAPC between November 2004 and October 2006 [12]. Although local control and survival did not reach significance in

☆ This study has not been presented previously.

* Corresponding author. Address: Department of Radiology, Hyogo Ion Beam Medical Center, 1-2-1 Kouto, Shingu-cho, Tatsuno, Hyogo 679-5165, Japan.
E-mail address: terashima@kmyr.jp (K. Terashima).

0167-8140/$ - see front matter © 2012 Elsevier Ireland Ltd. All rights reserved.
doi:10.1016/j.radonc.2011.12.029

comparison with other treatments, such as chemotherapy alone or CRT, we confirmed the feasibility and safety of proton radiotherapy. Based on this pilot study, we started gemcitabine-concurrent proton radiotherapy (GPT) for LAPC to assess the feasibility and efficacy of this regimen. To our knowledge, this is the first report on the clinical use of concurrent gemcitabine and proton radiotherapy for the treatment of pancreatic cancer.

Patients and methods

Patient eligibility

Patients with LAPC which was defined as borderline resectable cancer and unresectable cancer without distant metastases [28], that was cytologically or histologically confirmed to be adenocarcinoma, with an Eastern Cooperative Oncology Group (ECOG) performance status of 0–2, and were in adequate physical condition to tolerate chemotherapy were eligible for this study. Patients with a history of abdominal radiotherapy or previous treatment of pancreatic tumor were excluded.

All patients provided written informed consent prior to enrollment. The study was approved by the institutional review board and registered on the University Hospital Medical Information Network Clinical Trials Registry (UMIN-CTR, http://www.umin.ac.jp/ctr, UMIN ID: UMIN000002173).

Pretreatment workup

At baseline, all patients underwent an abdominal contrast-enhanced computed tomography (CT) scan, chest CT scan, positron emission tomography with ^{18}F-fluorodeoxy glucose (FDG-PET), and gastrointestinal fiberscopy (GIF) and were assessed for tumor markers (CA19-9, CEA, DUPAN-2, and SPAN-1). The disease was staged according to the International Union Against Cancer (UICC) TNM staging system, 6th edition.

Treatment regimen

Concurrent and adjuvant chemotherapy

In all protocols, all patients were scheduled to receive intra-venous infusion of gemcitabine (800 mg/m^2) for 30 min for the initial 3 weeks (days 1, 8, and 15) during 5 weeks of proton radiotherapy. We determined the dose of gemcitabine according to the studies by Casper et al. [3] and Burris et al. [1], and the schedule according to the study by Murphy et al. [20]. Gemcitabine was administered if the absolute granulocyte count was >2000/mm^3 and the platelet count was >70000/m^3 on the scheduled day.

Following GPT, all patients received systemic gemcitabine-based chemotherapy for as long as possible.

Proton radiotherapy

Hyogo Ion Beam Medical Center (HIBMC) treats patients with both proton and carbon-ion beams. We decided to use proton therapy for this study, because proton beams can be delivered to the target from any direction by using a rotating gantry so that irradiation of the GI tract is minimized. However, a rotating gantry is not available for carbon ion therapy. Furthermore, we anticipated that the administration of gemcitabine would have a sensitizing effect on proton therapy, as previously shown in human pancreatic cancer cells [5].

The patients were treated with 150–210 MeV proton beams. A respiratory gating system was used for all patients to irradiate the beam during the exhalation phase. Patient set-up was performed daily by subtraction of the 2 sets of orthogonal digital radiographs before irradiation. The translation and rotation of the patient detected by the positioning system were compensated for by adjustment of the treatment couch. The setup was continued until the bony landmarks on the digitally reconstructed radiographs agreed within 1 mm. The biologic effects of proton therapy at our institution were evaluated in vitro and in vivo. The relative biologic effectiveness (RBE) values were determined to be 1.1 by biologic experiments [11]. Because all tissues are assumed to have almost the same RBE, doses expressed in GyE are directly comparable to photon doses.

Treatment planning

Proton beam treatment plans were developed using a CT-based 3-dimensional treatment planning system. The gross tumor volume (GTV) was defined as the primary tumor plus the apparent lymph nodes as determined by a fusion contrast-enhanced CT subsidiary using FDG-PET. The clinical target volume (CTV) comprised the addition of a 5-mm margin to the GTV and prophylactic irradiation regions containing the draining lymph nodes and paraaortic lymph nodes as well as peripheral regions surrounding the celiac artery and superior mesenteric artery. We defined the CTV to contain the prophylactic region because metastases to regional lymph nodes have been recognized as prognostic factors in some studies of CRT [8] and resection [23,27] for LAPC. The planning target volume (PTV) was defined as the CTV plus a setup margin (5 mm) and a respiratory gating margin (1–5 mm), which was measured on CT images between inspiratory and expiratory phases. In general, the stomach, small bowel including the duodenum, kidneys, and spinal cord were defined as organs-at-risk (OAR). The dose restrictions for stomach, duodenum, and spinal cord were approximately 50 GyE, 50 GyE, and 45 GyE, respectively [13,14]. Additionally, we planned the irradiated volumes of the stomach, duodenum, and kidneys to be as small as possible.

Dose-fractionation

A total of 3 protocols were used in this study. In the early phase of the study, 2 protocols were used contemporaneously; protocol P-1 (50 GyE in 25 fractions) was used for patients with GI-adjacent LAPC, and P-2 (70.2 GyE in 26 fractions) was used for those with non-GI-adjacent LAPC. The non-GI-adjacent LAPC were defined as tumors that could be treated with irradiation plans that covered the GTV: over 95% of the prescribed dose in P-2 (70.2 GyE), which kept the dose administered to the GI-tract under 50 GyE. The others were defined as GI-adjacent LAPC who were treated with P-1. After the early phase, all patients were treated with protocol P-3 (67.5 GyE in 25 fractions) using the field-within-a-field technique.

In P-1, a total dose of 50 GyE was delivered in 25 fractions over 5 weeks to the PTV, based on our pilot study [12] and the report of 5-FU-concurrent CRT [19], in which irradiation doses of 39.6–50.4 Gy did not result in any late GI toxicity. In P-2, 70.2 GyE in 26 fractions over 6 weeks was delivered to the PTV. This approach was designed based on our experiences in treating head and neck cancers and lung cancer as well as other tumors, in which 70.2 GyE in 26 fractions was employed after dose escalation from 65 GyE in 26 fractions [21].

In P-3, 67.5 GyE in 25 fractions over 5 weeks was delivered using the field-within-a-field technique. With this technique, we used three types of split doses: 2 + 0.7 GyE, 1.8 + 0.9 GyE, and 1.6 + 1.1 GyE. For example, we delivered 1.8 GyE to the whole PTV (Fig. 1a) and 0.9 GyE to the PTV excluding the GI tract including stomach, small bowel, and large bowel, in one fraction (Fig. 1b). Consequently, a maximum dose of 2.7 GyE was administered as a single fraction (total 67.5 GyE) to the majority of the PTV (Fig. 1c), in parallel with limiting the dose to the GI tract to approximately

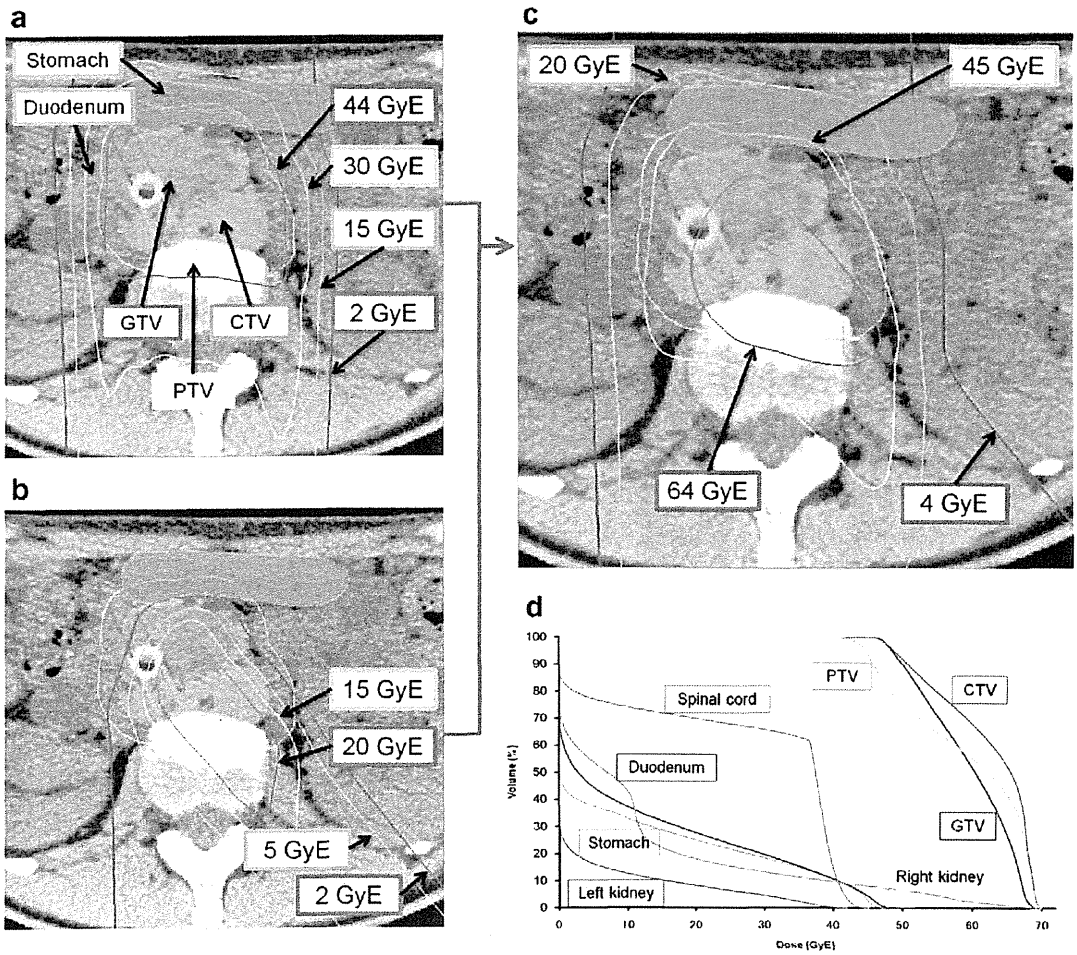

Fig. 1. A representative patient with locally advanced pancreatic cancer that was adjacent to the GI tract, treated with the gemcitabine-concurrent proton therapy (GPT) under protocol-3 (using the field-within a-field technique). (a) Dose distribution of the proton beam only at 1.8 GyE per fraction. A total dose of 45 GyE, which was the minimal dose administered to the PTV, was administered to the entire PTV. (b) Dose distribution at 0.9 GyE per fraction. A total dose of 22.5 GyE was irradiated to the PTV except for the GI tract (stomach and duodenum). (c) Summation of 1.8 GyE and 0.9 GyE in daily fractions. A total dose of 67.5 GyE was administered as the maximum dose, while the stomach and duodenum were only irradiated with approximately 45 GyE. (d) The dose–volume histogram of this plan for gross tumor volume (GTV), clinical target volume (CTV), planning target volume (PTV), and the organs-at-risk (stomach, duodenum, bilateral kidneys, and spinal cord).

1.8 GyE (total 45 GyE). With this technique, it became possible to treat all patients with the P-3 protocol alone, independent of GI-adjacency.

Follow-up

All patients received abdominal contrast-enhanced CT every three months and tumor marker monitoring every month after GPT. GIF was performed at the end of the GPT and every three-months thereafter to evaluate GI toxicity. Toxicity was assessed using the Common Terminology Criteria for Adverse Events (CTCAE) v3.0.

Comparison of the protocols

To clarify the characteristics and effectiveness of the field-within-a-field technique, we analyzed the treatment plans for proton therapy using a dose-volume histogram (DVH) and compared P-3 with P-1 and P-2 in terms of $D_{80\%}$, $D_{50\%}$, and $D_{20\%}$ ($D_{x\%}$ indicates the dose delivered to $x\%$ of the target volume) of the GTV, CTV, and PTV, as well as D_{max} (a maximum dose to the target) of the stomach and duodenum.

Evaluation of local control

As the radiographic changes caused by the GPT were not significant, local control was judged comprehensively by changes in the maximum tumor diameter, the inner density on contrast-enhanced CT, the levels of tumor markers including CA19-9 and CEA, which are particularly useful for pancreatic cancer [29], and the accumulation on FDG-PET. We conclusively defined local progression as radiographic enlargement of the primary tumor or locoregional recurrence or tendency to increase in tumor markers for at least three months without any distant metastases.

End points and statistical analysis

The primary end points were feasibility and toxicity, and the secondary end points were freedom from local progression (FFLP), progression-free survival (PFS), and overall survival (OS). These were estimated from the date of the GPT initiation to the date of the event or the last follow-up.

The FFLP, PFS, and OS rates were calculated using the Kaplan–Meier method. Unpaired Student's *t*-test was used to compare parameters of dose–volume histograms between the protocols.

Statistical analyses were carried out with SPSS Version 17.0 software (SPSS, Chicago, Illinois, USA).

Role of funding source

The sponsors of the study did not play any role in the study design, data collection, data analysis, data interpretation, or writing of the report.

Results

Patient and tumor characteristics

A total of 50 eligible patients with LAPC were enrolled in this study between February 2009 and August 2010. Five patients were enrolled in P-1, 5 in P-2, and 40 in P-3. The patient characteristics are summarized in Table 1.

The analyses of proton therapy performed using the dose–volume histogram (DVH) are shown in Table 2. When compared between P-1 (for non-GI-adjacent LAPC) and P-3 using Student's *t*-test, all of the parameters, except $D_{80\%}$ of the PTV, were significantly higher in P-3 than in P-1, even though P-3 included many patients with GI-adjacent LAPC. The comparison between P-2 and P-3 did not detect any significant difference. We could not find a significant difference for D_{max} of the stomach among P-1, P-2, and P-3. While there was a possibility that bias of tumor location (all 5 patients in P-2 had tumors in the body/tail of the pancreas) and tumor size (apparently smaller in P-2 than P-3) affected to the statistical result, the mean dose of D_{max} to the duodenum in P-3 was significantly lower than in P-2. These findings support the superiority of the field-within-a-field technique.

Adjuvant chemotherapy

Among 50 patients, 45 patients (90%) were able to continue adjuvant systemic gemcitabine-based chemotherapy after GPT. Five patients (10%) failed because of unacceptable toxicity of the adjuvant chemotherapy or rapid disease progression.

Feasibility and toxicity

P-1 and P-2 protocols

All 5 patients completed the scheduled GPT in P-1. Four patients completed treatment in P-2; 1 patient (20%) could not complete proton therapy at 62.1 GyE in 23 fractions due to gastric bleeding caused by acute radiation mucositis and was cured by medication only. There was no late toxicity in that case. In P-1 and P-2, hematologic toxicities were tolerable. The acute and late toxicities in all protocols are summarized in Table 3.

P-3 protocol

Of the 40 patients in P-3, 5 patients (13%) could not receive the third gemcitabine administration because of acute hematologic and GI toxicities. The most common toxicities were neutropenia, anorexia, and weight loss (Table 3).

The major late toxicities were gastric hemorrhage and ulcer. Late gastric ulcer with hemorrhage of grade 3 or greater was observed in 4 (10%) of 40 patients. All of them had pancreatic cancer arising in the body/tail of pancreatic region. Among these 4 patients, 3 patients (8%) were cured with medication (grade 3), but 1 patient (3%) died of gastric hemorrhage six months after GPT (grade 5). This death might have been related to the GPT because gastric ulcer and erosion were confirmed by GIF on the posterior wall of the lower gastric body 2 weeks prior to death. This patient had received the maximum dose of 52 GyE to the stomach.

Local control, distant metastases and survival

The one-year FFLP, PFS, and OS rates for all patients were 81.7% (95% CI: 65–99%), 64.3% (95% CI: 48–81%), and 76.8% (95% CI: 64–89%), respectively (Figs. 2 and 3), and 79.9% (95% CI: 58–100%), 60.8% (95% CI: 41–80%), and 78.8% (95% CI: 65–93%), respectively for patients treated with P-3. Of all 50 patients, local progression developed in only 4 patients (8%), while distant metastasis developed in 15 patients (30%), within one year. Frequent sites of distant metastasis were the liver in 9 patients (18%), lung in 1 patient (2%), and the peritoneum in 3 patients (6%). Five patients (10%) were already diagnosed with liver metastases at the end of GPT. None of

Table 1
Patient characteristics.

Characteristic	Protocol P-1 ($n = 5$)	Protocol P-2 ($n = 5$)	Protocol P-3 ($n = 40$)
Follow-up time, months			
Median (range)	12.3 (8.2–18.6)	19.6 (17.7–21.5)	12.1 (3.2–22.3)
Age, years			
Median (range)	57 (55–75)	56 (45–72)	64 (49–83)
Gender			
Male	3	2	18
Female	2	3	22
ECOG-PS			
0	2	3	27
1	3	2	10
2	0	0	3
UICC-TNM			
T3N1M0	0	1	4
T4N0M0	1	2	6
T4N1M0	4	2	30
Tumor location			
Head	1	0	18
Body/tail	4	5	22
Tumor size, cm			
Median (range)	4.6 (3.1–5.6)	3.2 (4.5–7.2)	3.7 (2.5–7)
CEA, ng/mL			
Median (range)	3.8 (1–12)	1.6 (1–6)	3 (0.9–16.4)
CA19-9, U/mL			
Median (range)	999 (0–6010)	73.2 (15–731)	185 (0–27600)

Abbreviations: ECOG, Eastern Cooperative Oncology Group; PS, performance status; UICC-TNM, the International Union Against Cancer (UICC) TNM staging system.

Table 2
Summary of proton therapy.

	P-1 50 GyE/25 fr Median (range), GyE	P-2 70.2 GyE/26 fr Median (range), GyE	P-3 67.5 GyE/25 fr Median (range), GyE	*t*-test (P-1, P-3) *P*-value	*t*-test (P-2, P-3) *P*-value
GTV $D_{80\%}$	49.9 (49.6–50)	58.2 (43.6–68.1)	53.4 (43.1–66.4)	<0.01	0.12
GTV $D_{50\%}$	50.2 (50–50.4)	64.4 (49.2–70.1)	61.1 (50.2–67.6)	<0.01	0.22
GTV $D_{20\%}$	50.6 (50.4–50.8)	66.6 (52.3–70.4)	66 (57.1–68.1)	<0.01	0.88
CTV $D_{80\%}$	49.9 (49.4–50.4)	56.1 (41.9–65.6)	52.5 (41.7–60)	<0.01	0.19
CTV $D_{50\%}$	50.3 (50–50.5)	64.4 (48.9–69.1)	62.6 (53.2–67.1)	<0.01	0.68
CTV $D_{20\%}$	50.7 (50.5–51)	66.6 (51.6–70.8)	67.4 (65.4–68.2)	<0.01	0.85
PTV $D_{80\%}$	49.7 (49.4–50.1)	51.6 (36.6–60.7)	49.4 (40.8–61)	0.72	0.42
PTV $D_{50\%}$	50.3 (50–50.5)	61.4 (46.2–67.6)	59.5 (46.3–66.5)	<0.01	0.50
PTV $D_{20\%}$	50.8 (50.6–51.2)	66.3 (50.8–70.4)	66.9 (63.1–68)	<0.01	0.89
Stomach D_{max}	51 (4–52)	46 (39–56)	48 (38–52)	0.52	0.54
Duodenum D_{max}	41 (40–46)	51 (51–52)	48.5 (42–52)	<0.01	<0.01

Abbreviations: GyE, gray equivalents; fr, fractions; GTV, gross tumor volume; CTV, clinical target volume; PTV, planning target volume; D_{xx}, dose delivered to *x*% of the target volume; D_{max}, maximum dose.

Table 3
Acute and late adverse events of grade 3 or greater.

Toxicity	P-1 ($n = 5$)		P-2 ($n = 5$)				P-3 ($n = 40$)							
	Acute		Acute		Late		Acute				Late			
	Grade 3		Grade 3		Grade3		Grade 3		Grade 4		Grade 3		Grade 5	
	n	(%)	*n*	(%)	*n*	(%)	*n*	(%)	*n*	(%)	*n*	(%)	*n*	(%)
Hematologic														
Leukopenia	1	(20)	3	(60)			15	(38)	1					
Neutropenia	1	(20)	2	(40)			9	(23)	2					
Anemia			1	(20)										
Thrombocytopenia			1	(20)			2	(5)						
Gastrointestinal														
Nausea							2	(5)						
Vomiting							1	(3)						
Anorexia	1	(20)	1	(20)			3	(8)			1	(3)		
Epigastralgia	1	(20)					2	(5)						
Gastric ulcer					1	(20)					3	(8)	1	(3)
Miscellaneous														
Weight loss							3	(5)						
Fatigue	1	(20)					1	(3)			1	(3)		

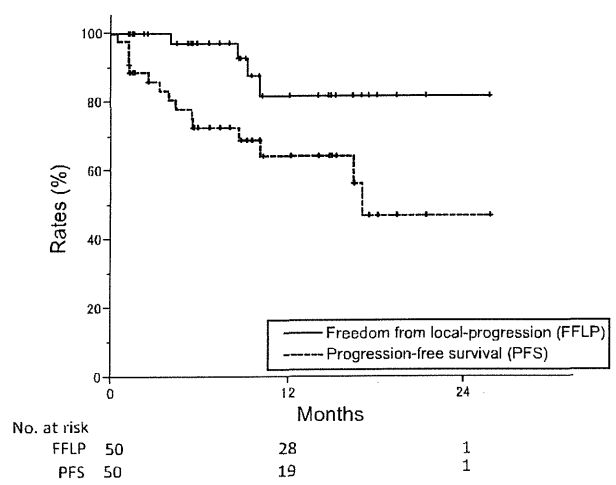

Fig. 2. The freedom from local-progression (solid line) and progression-free (dashed line) survival rates for all patients.

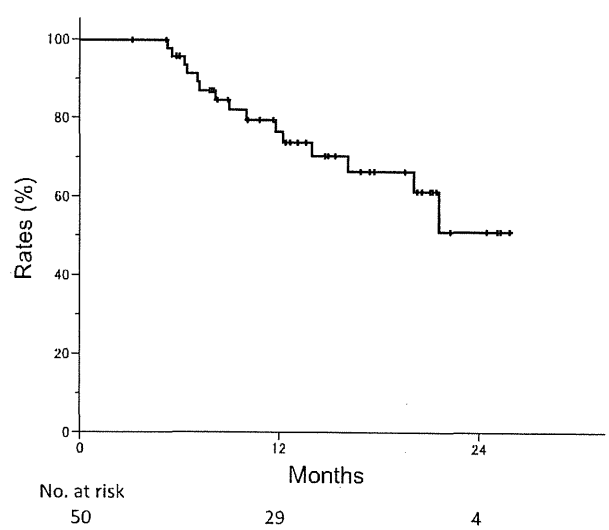

Fig. 3. The overall survival rate for all patients.

the patients died of local progression. One patient (2%) who developed both locoregional and distant metastases died of gastric hemorrhage (grade 5). Twelve patients (24%) have survived over 12 months to date without any signs of local or distant tumor progression.

Discussion

Our study indicated the high feasibility and tolerability of proton radiotherapy concurrently with high dose gemcitabine at 800 mg/m^2 on days 1, 8, and 15 during proton beam radiotherapy. The low frequency of grade 3 or greater acute GI toxicities, even at doses as high as 70.2 GyE (P-2) or 67.5 GyE (P-3), suggests superior dose localization of the proton beams to the target. However, late GI toxicities in P-3 (gastric ulcer and hemorrhage of grade 5) cannot be disregarded. We recognized that gastric peristalsis might bring unexpected high dose to the stomach, leading to severe complications in those patients, but it is a limitation of the current treatment planning technique. To prevent these major late toxicities, we have restricted irradiation doses to the GI tract by regulating the target fields and gantry angles and selecting an optimal split dose for the field-within-a-field technique. In contrast to the gastric toxicities, we did not encounter critical ulcer or hemorrhage in the duodenum, although it was irradiated at a dose similar to that of the stomach. The reason that no serious GI toxicity occurred in patients with pancreatic body/tail cancer seems to stem from the tolerability of the duodenum. As this lower frequency of duodenal toxicity is very interesting, we continued careful observation of the duodenum by duodenal fiberscopy.

From our clinical experience, it appears that the field-within-a-field technique that we used at P-3 enabled us to reduce the irradiation of OAR while maintaining the necessary doses to the PTV. Our analyses of the DVH indicate that using the field-within-a-field technique can increase the dose to the PTV of patients with GI-adjacent LAPC. Despite an increase in the dose to the PTV, the maximum dose to the stomach and duodenum was not increased. In addition, the optimal split dose of the field-within-a-field technique can be selected according to the tumor adjacency to the GI tract, so that the OAR are irradiated within a tolerable limit. Accordingly, GPT performed using the field-within-a-field technique contributed to solving of the mentioned three problems: reduction of irradiation dose, gemcitabine dose, and irradiation field.

Murphy et al. demonstrated that FFLP was a significant factor of OS on multivariate analysis [20]. To improve FFLP, our GPT was designed to deliver proton beams at a higher dose to a large CTV with concurrent administration of gemcitabine. As a result, the one-year FFLP and OS rates in our study were greater than expected, with high rates of 81.7% and 76.8%, respectively. This high FFLP rate is considered to be due to a large CTV, which was locally irradiated by proton beams at a high dose; thus, a good OS rate was achieved with low toxicities. However the one-year PFS rate was 64.3% which is low compared with the high FFLP and OS rates, this PFS rate is apparently better than that of other treatment modalities for patients with LAPC. Namely, the reported PFS rates are approximately 10–20% for CRT [7,17,22] and 10–15% for gemcitabine-based chemotherapy alone [1,9]. It is likely that the substantial local control of the primary tumor exerted by GPT decreased distant metastases and that the use of concurrent and adjuvant gemcitabine has contributed to the prolongation of life of patients with LAPC.

The one-year OS rate obtained in our study is apparently better than that obtained for patients treated with chemo-photon therapy [7,17,20]. Therefore, we consider that proton therapy using the field-within-a-field technique combined with concurrent gemcitabine or another promising chemotherapy has the potential to improve survival, including radical cure, for patients with LAPC.

Conclusions

GPT for LAPC was feasible and tolerable, and GPT using the field-within-a-field technique resulted in high FFLP and OS rates in our study. Although the number of patients enrolled in this study is too small and the follow-up periods are too short to draw any definitive conclusions, the clinical results obtained to date seem very encouraging.

Conflicts of interest

None.

References

[1] Burris 3rd HA, Moore MJ, Andersen J, et al. Improvements in survival and clinical benefit with gemcitabine as first-line therapy for patients with advanced pancreas cancer: a randomized trial. J Clin Oncol 1997;15:2403–13.
[2] Carpelan-Holmstrom M, Nordling S, Pukkala E, et al. Does anyone survive pancreatic ductal adenocarcinoma? A nationwide study re-evaluating the data of the Finnish Cancer Registry. Gut 2005;54:385–7.
[3] Casper ES, Green MR, Kelsen DP, et al. Phase II trial of gemcitabine (2,2′-difluorodeoxycytidine) in patients with adenocarcinoma of the pancreas. Invest New Drugs 1994;12:29–34.
[4] D'Souza MA, Shrikhande SV. Pancreatic resectional surgery: an evidence-based perspective. J Cancer Res Ther 2008;4:77–83.
[5] Galloway NR, Aspe JR, Sellers C, Wall NR. Enhanced antitumor effect of combined gemcitabine and proton radiation in the treatment of pancreatic cancer. Pancreas 2009;38:782–90.
[6] GITSG. Treatment of locally unresectable carcinoma of the pancreas: comparison of combined-modality therapy (chemotherapy plus radiotherapy) to chemotherapy alone. Gastrointestinal Tumor Study Group. J Natl Cancer Inst 1988;80:751–5.
[7] Huang PI, Chao Y, Li CP, et al. Efficacy and factors affecting outcome of gemcitabine concurrent chemoradiotherapy in patients with locally advanced pancreatic cancer. Int J Radiat Oncol Biol Phys 2009;73:159–65.
[8] Ikeda M, Okada S, Tokuuye K, Ueno H, Okusaka T. Prognostic factors in patients with locally advanced pancreatic carcinoma receiving chemoradiotherapy. Cancer 2001;91:490–5.
[9] Ishii H, Furuse J, Boku N, et al. Phase II study of gemcitabine chemotherapy alone for locally advanced pancreatic carcinoma: JCOG0506. Jpn J Clin Oncol 2010;40:573–9.
[10] Iwata H, Murakami M, Demizu Y, et al. High-dose proton therapy and carbon-ion therapy for stage I nonsmall cell lung cancer. Cancer 2010;116:2476–85.
[11] Kagawa K, Murakami M, Hishikawa Y, et al. Preclinical biological assessment of proton and carbon ion beams at Hyogo Ion Beam Medical Center. Int J Radiat Oncol Biol Phys 2002;54:928–38.
[12] Kamigaki T, Murakami M, Matsumoto IMM. A phase I study of proton beam therapy for locally advanced pancreatic cancer: analysis of feasibility and anti-tumor effect. J Clin Oncol 2008;26 [May 20 Suppl.; abstr 15675) 2008].
[13] Kavanagh BD, Pan CC, Dawson LA, et al. Radiation dose–volume effects in the stomach and small bowel. Int J Radiat Oncol Biol Phys 2010;76:S101–7.
[14] Kirkpatrick JP, van der Kogel AJ, Schultheiss TE. Radiation dose–volume effects in the spinal cord. Int J Radiat Oncol Biol Phys 2010;76:S42–9.
[15] Komatsu S, Fukumoto T, Demizu Y, et al. Clinical results and risk factors of proton and carbon ion therapy for hepatocellular carcinoma. Cancer 2011.
[16] Lawrence TS, Eisbruch A, McGinn CJ, Fields MT, Shewach DS. Radiosensitization by gemcitabine. Oncology (Williston Park) 1999;13:55–60.
[17] Li CP, Chao Y, Chi KH, et al. Concurrent chemoradiotherapy treatment of locally advanced pancreatic cancer: gemcitabine versus 5-fluorouracil, a randomized controlled study. Int J Radiat Oncol Biol Phys 2003;57:98–104.
[18] Moertel CG, Frytak S, Hahn RG, et al. Therapy of locally unresectable pancreatic carcinoma: a randomized comparison of high dose (6000 rads) radiation alone, moderate dose radiation (4000 rads + 5-fluorouracil), and high dose radiation + 5-fluorouracil: The Gastrointestinal Tumor Study Group. Cancer 1981;48:1705–10.
[19] Morganti AG, Valentini V, Macchia G, et al. 5-Fluorouracil-based chemoradiation in unresectable pancreatic carcinoma: phase I–II dose-escalation study. Int J Radiat Oncol Biol Phys 2004;59:1454–60.
[20] Murphy JD, Adusumilli S, Griffith KA, et al. Full-dose gemcitabine and concurrent radiotherapy for unresectable pancreatic cancer. Int J Radiat Oncol Biol Phys 2007;68:801–8.
[21] Nishimura H, Ogino T, Kawashima M, et al. Proton-beam therapy for olfactory neuroblastoma. Int J Radiat Oncol Biol Phys 2007;68:758–62.
[22] Okusaka T, Ito Y, Ueno H, et al. Phase II study of radiotherapy combined with gemcitabine for locally advanced pancreatic cancer. Br J Cancer 2004;91:673–7.

[23] Ozaki H, Hiraoka T, Mizumoto R, et al. The prognostic significance of lymph node metastasis and intrapancreatic perineural invasion in pancreatic cancer after curative resection. Surg Today 1999;29:16–22.
[24] Loehrer PJ, Powell ME, Cardenes HR, Wagner L, Brell JM, Ramanathan RK, et al. Eastern Cooperative Oncology Group. A randomized phase III study of gemcitabine in combination with radiation therapy versus gemcitabine alone in patients with localized, unresectable pancreatic cancer: E4201. J Clin Oncol 2008;26 [May 20 Suppl.; abstr 4506].
[25] Schulz.-Ertner D, Tsujii H. Particle radiation therapy using proton and heavier ion beams. J Clin Oncol 2007;25:953–64.
[26] Shinchi H, Takao S, Noma H, et al. Length and quality of survival after external-beam radiotherapy with concurrent continuous 5-fluorouracil infusion for locally unresectable pancreatic cancer. Int J Radiat Oncol Biol Phys 2002;53:146–50.
[27] Sohn TA, Yeo CJ, Cameron JL, et al. Resected adenocarcinoma of the pancreas-616 patients: results, outcomes, and prognostic indicators. J Gastrointest Surg 2000;4:567–79.
[28] Vincent A, Herman J, Schulick R, Hruban RH, Goggins M. Pancreatic cancer. Lancet 2011;378:607–20.
[29] Wong D, Ko AH, Hwang J, Venook AP, Bergsland EK, Tempero MA. Serum CA19-9 decline compared to radiographic response as a surrogate for clinical outcomes in patients with metastatic pancreatic cancer receiving chemotherapy. Pancreas 2008;37:269–74.

Utility of Contrast-Enhanced FDG-PET/CT in the Clinical Management of Pancreatic Cancer

Impact on Diagnosis, Staging, Evaluation of Treatment Response, and Detection of Recurrence

Akinori Asagi, MD, Koji Ohta, MD, PhD,† Junichirou Nasu, MD, PhD,* Minoru Tanada, MD,† Seijin Nadano, MD,* Rieko Nishimura, MD, PhD,‡ Norihiro Teramoto, MD, PhD,‡ Kazuhide Yamamoto, MD, PhD,§ Takeshi Inoue, MD, PhD,|| and Haruo Iguchi, MD, PhD**

Objectives: Fluorodeoxyglucose (FDG)–positron emission tomography/contrast-enhanced computed tomography (PET/CE-CT) involving whole-body scanning first by non–CE-CT and FDG-PET followed by CE-CT has been used for detailed examination of pancreatic lesions. We evaluated PET/CE-CT images with regard to differential diagnosis, staging, treatment response, and postoperative recurrence in pancreatic cancer.

Methods: Positron emission tomography/CE-CT was conducted in 108 patients with pancreatic cancer and in 41 patients with other pancreatic tumor diseases.

Results: The maximum standardized uptake value (SUV_{max}) overlapped in benign and malignant cases, suggesting that differential diagnosis of pancreatic tumors based on the SUV_{max} is difficult. In the evaluation of staging in 31 resectable pancreatic cancer by PET/CE-CT, the diagnostic accuracy rate was more than 80% for most factors concerning local invasion and 94% for distant metastasis but only 42% for lymph node metastasis. Significant positive correlations were found between the SUV_{max} and tumor size/markers, suggesting that SUV_{max} may be a useful indicator for the treatment response. Regarding the diagnosis of the postoperative recurrence, PET/CE-CT correctly detected local recurrence in all the 11 cases of recurrence, whereas abdominal CE-CT detected only 7 of 11 cases, suggesting that PET/CE-CT is superior in this context.

Conclusions: Positron emission tomography/CE-CT is useful for the clinical management of pancreatic cancer.

Key Words: contrast-enhanced PET/CT, differential diagnosis, clinical management, pancreatic cancer

(*Pancreas* 2013;42: 11–19)

Despite recent significant advances in cancer diagnosis and treatment, pancreatic cancer patients still have a very poor prognosis.[1] In Japan, the number of pancreatic cancer patients in 2002 was 21,386, whereas the number of pancreatic cancer–related deaths in 2006 was 23,366,[2] indicating that the number of patients with pancreatic cancer was almost equal to the number of pancreatic cancer–related deaths. However, a slight improvement in survival has been observed with the introduction of gemcitabine and S-1 as chemotherapeutic medications for pancreatic cancer.[3,4] Given this situation, clinical practice guidelines for pancreatic cancer have recently been established in Japan, and treatment regimens are determined on the basis of the extent of pancreatic cancer, which is evaluated by imaging. contrast-enhanced abdominal CT (abdominal CE-CT) has primarily been used to determine the extent of pancreatic cancer.[5] However, imaging diagnosis is also essential in the postoperative monitoring of pancreatic cancers, which often recur soon after surgery; abdominal CE-CT imaging has also been used for this purpose.

Positron emission tomography (PET), a new imaging modality, has recently been introduced in daily clinical practice, but functional imaging by PET alone does not have much diagnostic significance.[6] Acquisition of consecutive PET and CT (PET/CT) images in addition to combination of functional PET and anatomical CT images dramatically enhances the usefulness of PET as an imaging modality.[7] We have been using PET/CT (Aquiduo 16; Toshiba, Otawara, Japan) since the introduction of this technique at the Shikoku Cancer Center in April 2006; the CT apparatus has been dedicated to dynamic studies (contrast-enhanced PET/CT [PET/CE-CT]) on the development of this technique as a key imaging modality in the diagnosis and follow-up examinations of patients with pancreatic cancer. In this study, we retrospectively compared PET/CE-CT and abdominal CE-CT, which has been used as the primary imaging modality for the diagnosis and management of pancreatic cancer, and evaluated the efficacy of these modalities for the following functions: differential diagnosis of benign and malignant pancreatic lesions, evaluation of the extent of invasive pancreatic ductal cancer, assessment of treatment effects, and diagnosis of postoperative recurrence.

MATERIALS AND METHODS

Subjects

Positron emission tomography/CE-CT imaging technology was used to determine the extent of invasive pancreatic ductal cancer in 108 patients (64 men and 44 women, aged 45–86 years). The extent of cancer was determined according to the *Classification of Pancreatic Carcinoma, Fifth Edition* (edited by the Japan Pancreas Society [JPS]).[8] Among the 108 subjects, operations were performed on 29 patients with locally advanced pancreatic ductal cancer, and histologic diagnosis was proven in these patients. The remaining patients were diagnosed on the basis of PET/CE-CT imaging findings and serum tumor marker values.

From the Departments of *Gastroenterology, †Gastroenterological Surgery, and ‡Pathology, Shikoku Cancer Center, Ehime; §Department of Gastroenterology and Hepatology, Okayama University Graduate School of Medicine, Okayama; and ||Department of Diagnostic Radiology, Shikoku Cancer Center, Ehime, Japan.

Received for publication May 25, 2011; accepted March 5, 2012.

Reprints: Haruo Iguchi, MD, PhD, Department of Gastroenterology, Shikoku Cancer Center, Minami-Umemotomachi Ko 160, Matsuyama, Ehime 791-0280, Japan (e-mail: higuchi@shikoku-cc.go.jp).

The authors declare no conflict of interest.

This work was supported in part by a Grant-in-Aid for Research on Applying Health Technology (grant no. H23-Cancer-General-010) from the Ministry of Health, Labor, and Welfare of Japan and Management Expenses Grants (grant no. 22-54) from the Japanese government to the National Cancer Center.

Positron emission tomography/CE-CT imaging was conducted for relevant pancreatic tumor lesions to assess the usefulness of the maximum standardized uptake value (SUV_{max}) in differentiating benign and malignant pancreatic lesions. The SUV_{max} was the value obtained at 90 minutes after intravenous injection of fluorodeoxyglucose (FDG) in subjects with blood glucose levels of 200 mg/dL or less at the time of FDG administration.

Differential diagnosis for malignant and benign pancreatic disorders by PET/CE-CT imaging was performed in 21 patients with intraductal papillary mucinous neoplasm (IPMN; 9 men and 12 women, aged 47–78 years), in 10 patients with endocrine tumors of the pancreas (2 men and 8 women, aged 42–78 years), and in 10 patients with tumor-forming pancreatitis (chronic pancreatitis [CP] or autoimmune pancreatitis [AIP]; 8 men and 2 women, aged 40–79 years) in addition to the 108 patients with invasive pancreatic ductal cancer. Among the 21 patients with IPMN, 8 patients underwent operations, and the diagnosis of malignant tumors (intraductal papillary mucinous carcinoma [IPMC]) and benign tumors (intraductal papillary mucinous adenoma [IPMA]) was histologically proven in these patients. The remaining 13 patients were diagnosed with benign tumors (IPMA) based on the findings from imaging studies (PET/CE-CT, magnetic resonance imaging, and ultrasound), including branch type, lack of internal structures, and lack of FDG uptake. These patients are currently being observed by follow-up at more than 1 year after diagnosis. Ten patients with endocrine tumors of the pancreas were diagnosed based on the presence of hypervascular tumors with FDG accumulation on PET/CE-CT imaging. Among these patients, 7 underwent operations, and biopsies were performed in the remaining 3 patients, resulting in histologically proven diagnoses for all 10 patients. Malignancy and benignancy were determined based on histologic findings and by taking into account the presence or absence of metastatic lesions on the images. Chronic pancreatitis and AIP were diagnosed using PET/CE-CT imaging and serum levels of pancreatic enzymes and/or IgG4 according to the Diagnostic Criteria for Chronic Pancreatitis[9] 2002 and the Diagnostic Criteria for Autoimmune Pancreatitis 2006 (JPS).[10]

Classification of Pancreatic Cancer

In this study, we used the classification system for pancreatic cancer defined by the JPS.[8] According to the JPS classification system, the extent of invasive pancreatic ductal cancer was determined by taking into account local spread (T), lymph node metastases (N), and distant metastases (M). The T category was defined through determination of the presence and extent of local invasion of the pancreas and adjacent structures. Within this category, 8 local extension factors were considered: the distal bile duct (CH), duodenum (DU), serosa (S), retropancreatic tissue (RP), portal vein system (PV), arterial system (A), extrapancreatic nerve plexus (PL), and other organs (OO). The N category (lymph node metastases) was divided into 4 categories (N0-N3) according to whether metastasis was present in lymph nodes with groups 1 to 3. The presence of distant metastatic lesions, including metastasis to distant organs, the peritoneum, and group 3 lymph nodes, were defined as M1. On the basis of the grading for T, N, and M categories, tumor stage was divided into 5 groups, as shown in Fig. 1. A detailed description of stage grouping by JPS guidelines is described in a previous report by Isaji et al.[8]

PET/CT Imaging Protocol

All FDG-PET/CT studies were performed using an Aquiduo PET/CT scanner (Toshiba), which is a hybrid PET and 16-multidetector CT scanner. Patients fasted for at least 4 hours before the PET/CT examination. In all patients, blood glucose levels were checked before injection of the radiopharmaceutical. Intravenous injection of 3.0 MBq/kg body weight of FDG was followed by a 10-mL normal saline flush. Patients rested for approximately 90 minutes, during which time they were asked to drink 500 mL of a Japanese tea containing 5 mL of oral contrast medium (Gastrografin; Bayer Schering Pharma, Leverkusen, Germany) before image acquisition and to void before being positioned supine on the scanner table. Non–contrast-enhanced CT was performed first, from the vertex of the skull through the mid thigh at 80 to 200 mA s, 120 kV (peak) (kV[p]), and 2.0-mm collimation. Images were reconstructed as contiguous 4-mm slices. Positron emission tomography was performed immediately after non–contrast-enhanced CT without repositioning the patient. Positron emission tomography images were obtained at 7 to 8 stations per patient, with an acquisition time of 2 to 3 minutes per station, from the skull vertex through the mid thigh. The non–contrast-enhanced CT data were used for attenuation correction of PET emission images, which were coregistered with the non–contrast-enhanced CT data set. Then, dual-phase CE-CT was performed. Arterial-phase CT images were obtained 35 seconds after injection of 100 mL of iopamidol (Iopamiron 300; Bayer Schering Pharma). Contrast material was injected at 3 mL/s using a powder injector (Dual Shot GV; Nemoto, Tokyo, Japan). Arterial-phase images were obtained from the dome of the diaphragm to the iliac crest at 80 to 200 mA s, 120 kV(p), and 1.0-mm collimation. Arterial-phase images were reconstructed as contiguous 2-mm slices. Portal venous phase images were acquired after a delay of 90 seconds from the vertex of the skull through the mid thigh at 80 to 200 mA s, 120 kV(p), and 2.0-mm collimation. Portal venous phase images were reconstructed as contiguous 2-mm slices.

Positron emission tomography/CT imaging using this protocol (PET/CE-CT) can cover all angles of the diagnosis, including diagnosis of existing tumors, qualitative diagnosis, local diagnosis, and metastasis detection.

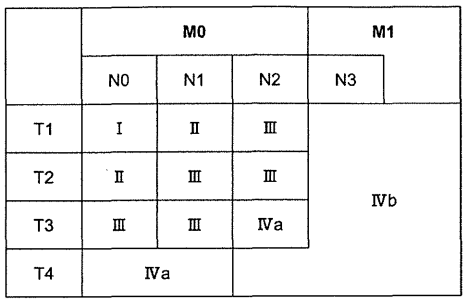

FIGURE 1. Stage grouping of pancreatic cancers according to JPS guidelines.[8] Stages of pancreatic cancer are grouped into 5 categories according to the cancer extent based on the grading of T, N, and M factors.

Evaluation of the Extent of Invasive Pancreatic Ductal Cancer

Operations were performed on 29 patients with locally advanced pancreatic ductal cancer (stage IVa), and diagnoses were histologically proven in these patients. Postoperatively, findings from PET/CE-CT imaging of the preoperative cancer were compared with the histologic findings of the resected specimens to determine the diagnostic accuracy rate of PET/CE-CT imaging for the evaluation of the extent of cancer progression. The degree of preoperative and postoperative cancer progression

was determined according to the JPS classification system.[8] In another 4 patients with invasive pancreatic ductal cancer, whose preoperative stage was diagnosed as resectable IVa by PET/CE-CT, only metastatic tissue biopsies were performed because distant metastases were found after initiation of the surgical procedure (lymph node [N3], 2 cases; liver, 1 case; peritoneum, 1 case). Thus, N and M categories were examined in 31 patients with stage IVa after the addition of these 2 cases. We also compared the diagnostic accuracy rate of PET/CE-CT imaging with that of abdominal CE-CT imaging, which was extracted from the PET/CE-CT imaging, for evaluating the extent of cancer.

We further evaluated the diagnostic accuracy rate of PET/CE-CT for M factor analysis in 65 patients with stage IVb unresectable pancreatic cancer because distant metastases are not normally found in stage IVa resectable pancreatic cancer, and compared it with that of CE-CT images, which were extracted from the PET/CE-CT images. In this analysis, the reference standard for the presence of distant metastases was based on multimodality images and follow-up observations because distant metastases were not histologically proven.

To compare the diagnostic accuracy rates of PET/CE-CT and abdominal CE-CT in the context of evaluating T, N, and M factors, 2 radiologists were asked to analyze sections from these images independently, without knowledge of the results of the other imaging. If a disagreement occurred, a final decision was made after a discussion of the radiologists' analyses.

Assessment of Treatment Effects

The effects of treatment were evaluated over time in 8 patients who had undergone chemotherapy or chemoradiotherapy for unresectable locally advanced pancreatic cancer, diagnosed using PET/CE-CT imaging (tumor diameter determined by CT and SUV_{max} determined by PET) and serum tumor marker levels (CA 19-9). After determining the rate of increases and decreases in tumor diameter, SUV_{max} values and CA 19-9 levels were assessed, and correlations among these factors were examined. This analysis was conducted only on patients whose pancreatic cancer was locally confined during the ongoing treatment and was discontinued whenever distant metastasis occurred. At each evaluation of treatment effectiveness, the change rate of each variable was calculated and examined for correlations. Therefore, although 8 patients were analyzed, the number of analyzable events was 12 because multiple events occurred per case.

Diagnosis of Postoperative Recurrence

Although pancreatic cancer often recurs soon after surgery, the anatomical positional relationship between various abdominal organs may be changed by surgery; therefore, an abdominal CE-CT scan alone is often insufficient for diagnosis of local recurrence, not to mention distant metastasis. In the present study, PET/CE-CT images were used to show postoperative recurrence in 11 patients and a lack of postoperative recurrence of invasive pancreatic ductal cancer in 6 patients. Local recurrence was diagnosed by PET/CE-CT based on the findings of soft tissue density mass with FDG accumulation, whereas soft tissue density mass without FDG accumulation was diagnosed as a postoperative change. The diagnosis of local recurrence by abdominal CE-CT, on the other hand, requires not only the presence of soft tissue density mass but also the ability to compare the mass with the size with the previously measured mass. Thus, an increase in the size of the soft tissue density mass was considered a local recurrence, whereas no increase and/or little increase in size were considered a lack of local recurrence. However, there are no standard criteria defining the increase in size that would constitute a local recurrence; thus, the diagnosis of local recurrence depends on the radiologist. In our cancer center, PET/CE-CT is usually conducted on patients in whom the serum levels of tumor markers are elevated during the follow-up period. To determine the diagnostic accuracy rate of abdominal CE-CT for the evaluation of local recurrence, 2 radiologists were asked to read only sections from abdominal CE-CT scans extracted from PET/CE-CT imaging independently, without knowledge of the results of other imaging findings. If a disagreement occurred, a final decision was made after discussion between the radiologists. Then, the diagnostic accuracy rate for local recurrence was compared between PET/CE-CT and abdominal CE-CT imaging. Although local recurrences were not histologically proven, they were confirmed by follow-up observations after the initial diagnosis by PET/CE-CT. As a result, the diagnostic accuracy rate of PET/CE-CT was 100%.

Statistical Analysis

Differences between the SUV_{max} values in various pancreatic disorders with tumorous lesions were evaluated using the *t* test. Differences in the diagnostic accuracy rates of the tested imaging modalities (PET/CE-CT and abdominal CE-CT) were evaluated using the Cochran Q test. Relationships between changes in tumor size (Ts), SUV_{max} values, and serum CA 19-9 levels during treatment were evaluated using linear regression analysis. $P < 0.05$ was considered statistically significant.

RESULTS

Differential Diagnosis of the Malignancy and Benignancy of Pancreatic Lesions by PET/CE-CT Imaging

Fig. 2 shows the SUV_{max} of various pancreatic tumor diseases. The SUV_{max} (mean [SD]) of invasive pancreatic ductal cancer was 6.14 (3.51) in stages I to III, 6.28 (2.91) in stage IVa, and 7.22 (2.65) in stage IVb; thus, the values for different stages were not significantly different. However, the SUV_{max} of invasive

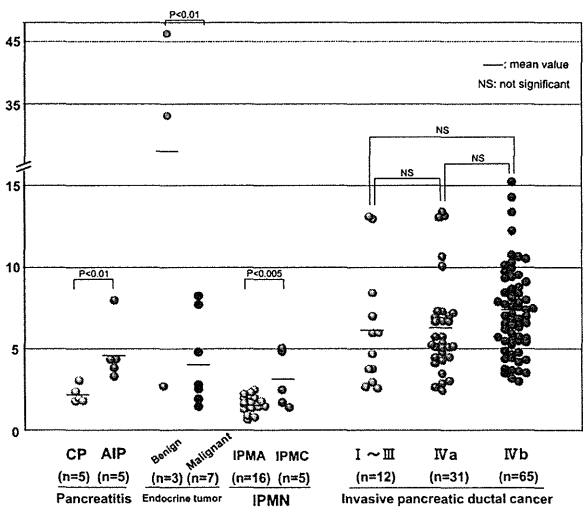

FIGURE 2. The SUV_{max} of different pancreatic tumor lesions. Ninety minutes after FDG infusion in various pancreatic tumor cases, PET/CE-CT scans were obtained to determine the SUV_{max}. Patients with blood glucose levels of 200 mg/dL or less at the time of FDG infusion were evaluated.

pancreatic ductal cancer tended to be higher than those of other pancreatic tumor diseases, excluding benign pancreatic endocrine tumors. In the case of IPMN, the SUV_{max} values (mean [SD]) were 3.09 (1.53) for IPMC (n = 5) and 1.59 (0.52) for IPMA (n = 16). The SUV_{max} of IPMC was significantly higher than that of IPMA ($P < 0.005$). In the case of pancreatic endocrine tumors, the SUV_{max} values (mean [SD]) were 27.4 (18.2) in benign cases (n = 3) and 4.21 (2.56) in malignant cases (n = 7); thus, the SUV_{was} markedly higher in benign cases. Among 3 cases of benign endocrine tumors, 2 cases exhibited extremely high SUV_{max} values, 33.5 and 46.1, and the histologic diagnosis for these cases was well-differentiated endocrine tumor with uncertain behavior according to the World Health Organization's classification of endocrine tumors published in 2004.[11] These 2 cases have been followed up for more than 3 years, and recurrence was not noted until August 2011. In tumor-forming chronic pancreatitis (n = 5) and tumor-forming AIP (n = 5), SUV_{max} values (mean [SD]) were 2.19 (0.48) and 4.76 (1.64), respectively; therefore, the SUV_{max} of AIP was significantly higher than that of chronic pancreatitis ($P < 0.01$).

Diagnostic Accuracy Rate of PET/CE-CT Imaging for Determining the Extent of Invasive Pancreatic Ductal Cancer

The diagnostic accuracy rate of PET/CE-CT for T, N, and M factor in patients with stage IVa resectable pancreatic cancer is shown in Table 1.

With respect to the T factor, the diagnostic accuracy rate of PET/CE-CT imaging for Ts, S, and RP was below 80%, although it was greater than 80% for CH, DU, PV, A, PL, and OO. Among these factors in the T category, A, PV, and PL are important to determine whether the locally advanced pancreatic cancer (stage IVa) is resectable. The diagnostic accuracy rates of A, PV, and PL were 97%, 86%, and 83%, respectively. Evaluation of the T factor by PET/CE-CT was based on the findings of the CE-CT images; therefore, the diagnostic accuracy rate of PET/CE-CT for the T factor was identical to that of abdominal CE-CT (data not shown).

Abdominal CE-CT imaging was used to determine the extent of N factor based on the shape and size of lymph nodes, whereas FDG uptake was used as an additional evaluation element in PET/CE-CT imaging (Fig. 3). The accuracy rate of PET/CE-CT for the N factor was 42% (Table 1A), whereas that of abdominal CE-CT was 35% in 31 patients with stage IVa resectable pancreatic cancer (data not shown). The breakdown of differentially diagnosed N factor characteristics as measured by PET/CE-CT and histologic examination (n = 18) is shown in Table 1B. Among these N factor diagnoses, overestimation and underestimation of the extent of N factor characteristics by PET/CE-CT were observed in 6 and 12 patients, respectively. In the 6 cases of overestimation, 4 were determined to be stage IVb unresectable cases solely based on the preoperative evaluation of N2 or N3 by PET/CE-CT. In the 12 cases of underestimation, on the other hand, 9 with peripancreatic lymph node metastasis in the resected specimen, which is histologically diagnosed as N1, were included.

With respect to the M factor, the diagnostic accuracy rate of PET/CE-CT imaging was 94% in 31 patients with stage IVa resectable pancreatic cancer (Table 1A). Two metastatic cases, one with metastasis to the surface of the liver and the other with miliary nodules of peritoneal dissemination, were not detected by the preoperative PET/CE-CT. We also evaluated the diagnostic accuracy rate of PET/CE-CT for M factor characteristics in 65 patients with stage IVb unresectable pancreatic cancer (Table 2). Lymph node metastasis (N3), hepatic metastasis, and peritoneal dissemination, which are often observed as distant metastasis of pancreatic cancer, were detected in 51%, 55%, and 53% of patients by PET/CE-CT and 45%, 53%, and 31% of cases by abdominal CE-CT, respectively. The detection rates of abdominal CE-CT for lymph node metastasis (N3) and peritoneal dissemination were significantly lower than that of PET/CE-CT, although the detection rate of hepatic metastasis was

TABLE 1. (A) Diagnostic Accuracy Rate of PET/CE-CT Imaging in Determining the Extent of Cancer in 31 Patients With Preoperative Stage IVa Resectable Pancreatic Cancer and (B) Breakdown of the Differently Diagnosed Extent of the N Factor With PET/CE-CT Imaging and Histologic Examination in 18 of 31 Patients With Preoperative Stage IVa Resectable Pancreatic Cancer

(A) PET/CE-CT*		(B) Extent of N Factor		
		PET/CT Imaging	Histologic Examination	No. Cases (n = 18)
T factor		N3, N2	→N1	4
Ts	14/28 (50%)	N1	→N0	2
CH	24/29 (83%)	N0	→N1	9
DU	26/29 (90%)	N0	→N2	1
S	22/29 (76%)	N0	→N3	2
RP	19/29 (66%)			
PV	25/29 (86%)			
A	28/29 (97%)			
PL	24/29 (83%)			
OO	29/29 (100%)			
N factor	13/31 (42%)			
M factor	29/31 (94%)			

*The extent of cancer was determined with regard to local spread (T), lymph node metastasis (N), and distant metastasis (M) according to the classification guidelines for pancreatic carcinomas published by the JPS.[8] Preoperative cancer extent diagnosed by PET/CE-CT imaging and histologic examination of resected specimens were compared among 29 patients with stage IVa resectable pancreatic cancer to calculate the diagnostic accuracy rate of PET/CE-CT imaging. Ts was not assessable in 1 resected specimen; therefore, Ts was determined in 28 specimens. Distant metastases were histologically proven in 4 more cases (2 lymph node [N3], 1 hepatic, and 1 peritoneal metastasis), in addition to 29 patients with stage IVa resectable pancreatic cancer, in whom only tissue biopsies were performed after initiation of the surgical procedure. These 4 cases were included in N and M factor evaluation; therefore, N and M factors were histologically determined in 31 specimens.

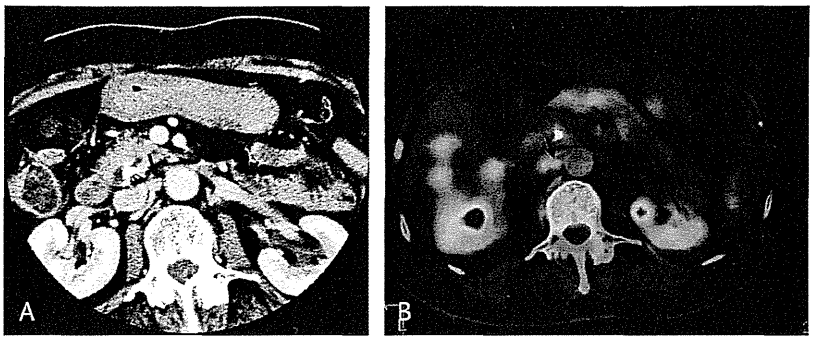

FIGURE 3. Positron emission tomography/CE-CT findings of a typical case (86-year-old woman) with lymph node metastasis. The CE-CT image shows no. 16b1 lymph node swelling (10.5 × 5.0 mm, flat shape); however, lymph node metastasis was ruled out based on the size and shape of the swelling as determined by CT (A). The PET/CT image, on the other hand, shows abnormal FDG uptake (SUV_{max}, 2.61) corresponding to this lymph node (B), suggesting lymph node metastasis. Histologic examination of the surgical specimen proved the involvement of lymph node lesions.

similar between the 2 methods. Lung and bone metastasis have rarely been detected by abdominal CE-CT because this type of imaging scans only a segmental area. Positron emission tomography/CE-CT imaging, on the other hand, scans the whole body, resulting in higher detection rates of lung and bone metastases (Table 2).

Assessment of Treatment Effects by PET/CE-CT Imaging

Unresectable pancreatic cancer is treated with chemotherapy or chemoradiotherapy, and the effectiveness of treatment is assessed according to RECIST guidelines[12] by determining the longest diameter of the measurable lesion, which is usually measured using abdominal CE-CT, and levels of serum tumor marker.

We determined the increase/decrease ratios of Ts, CA 19-9 levels, and SUV_{max} in the progressive disease and partial response groups. In contrast to small changes in Ts, the changes in CA 19-9 levels and SUV_{max} values were larger, and the patterns of changes in these indicators were similar (Fig. 4A). Among these 3 indicators, a significant positive correlation was found between SUV_{max} and CA 19-9 levels ($P < 0.0001$) and between SUV_{max} and Ts ($P < 0.05$), but no significant correlation was found between CA 19-9 levels and Ts (Fig. 4B).

TABLE 2. Difference Between PET/CE-CT and Abdominal CE-CT in the Diagnosis of the Extent of M Factor Progression in 65 Patients With Stage IVb Unresectable Pancreatic Cancer

	PET/CE-CT	Abdominal CE-CT
Lymph node (N3)	33 (51%)	29 (45%)*
Liver	36 (55%)	35 (53%)
Peritoneum	35 (53%)	20 (31%)†
Lung	12 (18%)	5 (8%)†
Bone	16 (24%)	3 (5%)†

Positron emission tomography/CE-CT was conducted at the time of diagnosis in 65 patients. The portions that correspond to the abdominal CE-CT were extracted from the PET/CE-CT images and reconstructed. Then, 2 radiologists assessed the extent of M factor characteristics on these extracted images. If a disagreement occurred, a final decision was made after discussion between the radiologists.

*$P < 0.05$ versus PET/CE-CT.

†$P < 0.01$ versus PET/CE-CT.

Diagnosis of Postoperative Recurrence

In patients with pancreatic cancer, recurrence is frequently observed shortly after the operation[13]; thus, diagnosis of recurrence is crucial for starting an appropriate treatment. Abdominal CE-CT is generally used for this diagnosis; however, in some cases, local recurrence may be difficult to detect because of postoperative alterations in the anatomical positions of visceral organs.[14,15] Therefore, we compared the rates of postoperative local recurrences diagnosed by abdominal CE-CT and PET/CE-CT imaging. Abdominal CE-CT detected 7 of the 11 cases diagnosed by PET/CE-CT imaging, and in 6 cases diagnosed as not having local recurrence by PET/CE-CT imaging, 5 cases were diagnosed correctly by abdominal CE-CT (Table 3). Typical findings from imaging of local recurrences by PET/CE-CT are shown in Fig. 5.

DISCUSSION

Preoperative evaluation of the extent of pancreatic cancer is important in deciding treatment options, and abdominal CE-CT is usually used for this purpose. In the present study, we determined the diagnostic accuracy rate of PET/CE-CT in evaluating the extent of pancreatic cancer and compared it to that of abdominal CE-CT. The accuracy rate for diagnosing the T factor, which includes an evaluation of local spread or invasion into the area surrounding the pancreas, was less than 80% for Ts, S, and RP and greater than 80% for the CH, DU, PV, A, PL, and OO. Among these factors, PV, A, and PL are important in deciding whether the tumors are resectable or not, and the accuracy rates of PET/CE-CT for these factors (PV, 86%; A, 97%; and PL, 87%) were satisfactory. The accuracy rate of abdominal CE-CT imaging for the T factor was identical to that of PET/CE-CT imaging because the CE-CT portion is the main evaluation tool for T factor analysis even on PET/CE-CT imaging. With respect to the N factor, Higashi et al[16] reported that the diagnostic accuracy rate assessed by CT images was not satisfactory. Zimny et al[17] reported a low accuracy rate for FDG-PET in evaluation of the N factor as well. In the present study, the diagnostic accuracy rate of PET/CE-CT for the N factor was 42%, despite the fact that the diagnosis was based on both CT images of the size and shape of lymph nodes and FDG uptake on PET, whereas the diagnostic accuracy rate of abdominal CE-CT was even

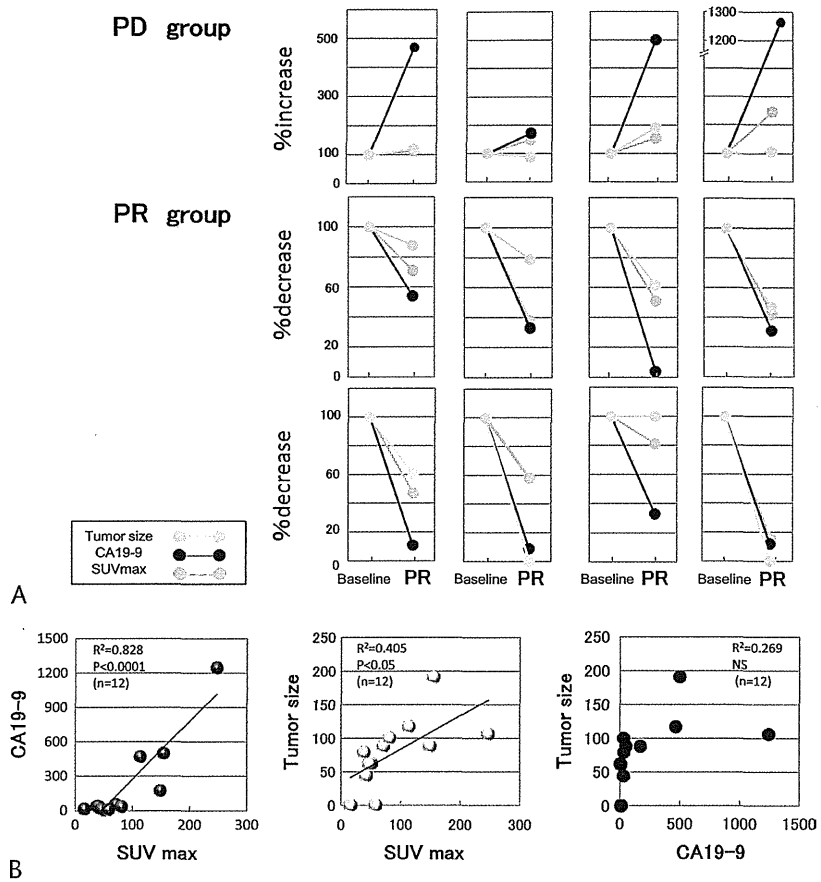

FIGURE 4. Monitoring treatment effectiveness in invasive pancreatic ductal cancer by PET/CE-CT. Chemotherapy or chemoradiotherapy was conducted in 8 patients with unresectable locally advanced pancreatic cancer. Positron emission tomography/CE-CT imaging (SUV_{max} by PET and Ts by CE-CT) and levels of serum tumor markers (CA 19-9) were used to assess the effects of treatment over time. Only tumors that were found to be locally confined during treatment were analyzed. Cases in which distant metastasis occurred were excluded from analysis. A, Changes in Ts, CA 19-9, and SUV_{max} during treatment. Compared with the baseline values (100%), the values at partial response or progressive disease are indicated by the percent decrease or increase. B, Correlations between the rate of change in Ts, CA 19-9, and SUV_{max} during treatment. NS indicates not significant.

lower (35%). The extent of the N factor was differentially diagnosed with PET/CE-CT and histologic examination in 18 cases; however, of these 18 cases, 9 cases of group 1 lymph node metastasis were diagnosed as N0 on PET/CE-CT but as N1 by histologic examination. These lymph nodes were attached to the resected specimens; therefore, detection of such lymph node metastasis by imaging seems impossible because of their small size and/or their merging with pancreatic tumors. If these 9 cases were excluded from our calculation of the diagnostic accuracy rate, the accuracy rate of PET/CE-CT for the N factor would be 13 (59%) of 22, although even this level is low. These results indicate that PET/CE-CT imaging is not very useful for assessing

TABLE 3. Positron Emission Tomography/CE-CT Versus Abdominal CE-CT for the Diagnosis of Postoperative Local Recurrence

		PET/CT	
		Recurrence (n = 11)	**No Recurrence (n = 6)**
CT	Recurrence	7	1
	No recurrence	4	5
	Accuracy rate	63%	83%

Shown are 11 cases diagnosed as "local recurrence" and 6 cases diagnosed as "no recurrence" by PET/CE-CT imaging during the postoperative monitoring period. The portion that corresponds to the abdominal CE-CT was extracted from PET/CE-CT images and reconstructed. Local recurrence was diagnosed by PET/CE-CT based on the findings of soft tissue-density mass with FDG accumulation, whereas soft tissue density mass without FDG accumulation was diagnosed as a postoperative change. The diagnosis of local recurrence by abdominal CE-CT, on the other hand, required not only the presence of soft tissue density mass but also the comparison of the current Ts with the previous measure of Ts. Two radiologists assessed local recurrence on these extracted images. If a disagreement occurred, a final decision was made after discussion between the radiologists.

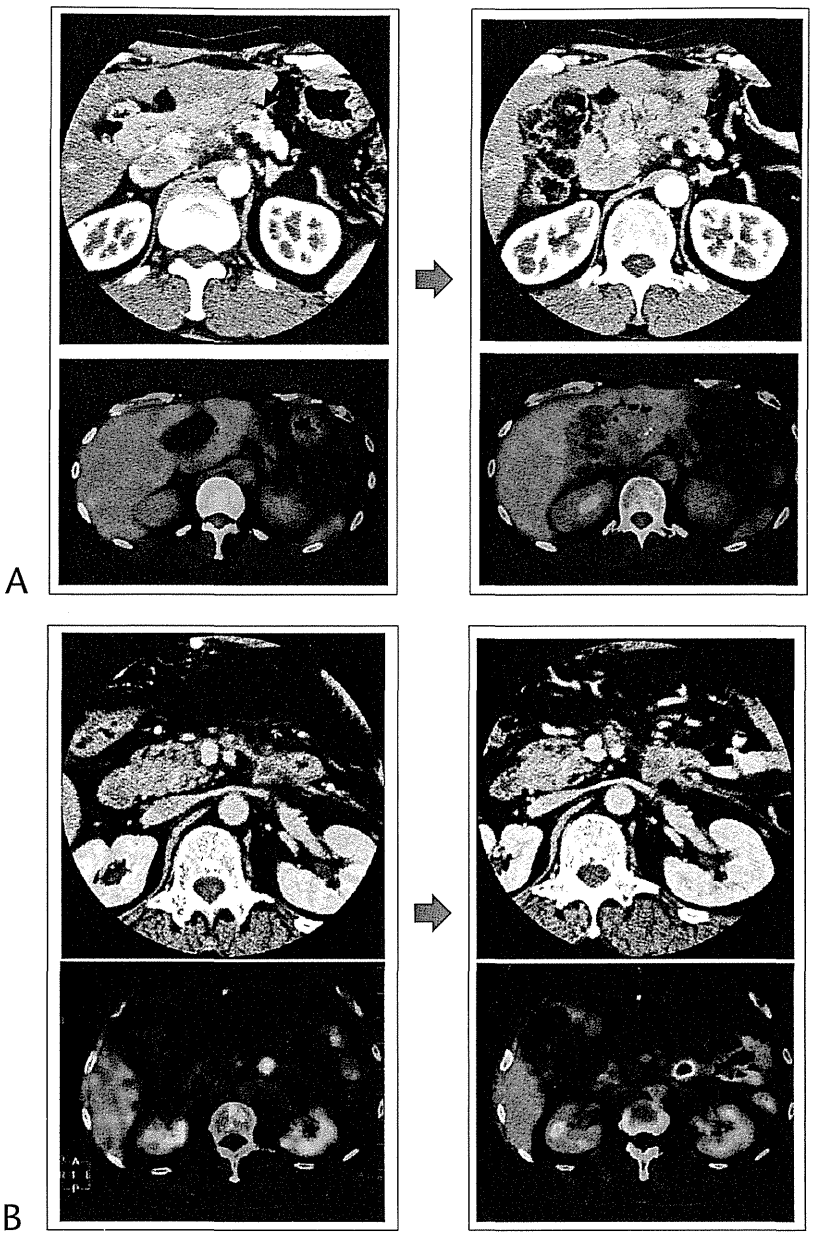

FIGURE 5. Positron emission tomography/CE-CT findings of 2 typical cases, 1 with "local recurrence" and the other with "no local recurrence," are shown. A, A 46-year-old man with no local recurrence (false-positive by CE-CT and true-negative by PET/CE-CT). The CE-CT image, which was performed 17 months after surgery, showed a soft tissue density mass, which did not rule out local recurrence (left upper panel, arrow). However, the PET/CT image did not show FDG uptake corresponding to this mass, suggesting no local recurrence (left lower panel, arrow). A follow-up PET/CE-CT image, which was performed 8 months after the initial examination, revealed no increase in the size and FDG uptake of the mass (right panel, arrow), indicating that the initial diagnosis of no local recurrence by PET/CE-CT was correct. B, A 59-year-old man with local recurrence (true-positive by CE-CT and PET/CE-CT). The CE-CT image, which was performed 3 months after surgery, showed a soft tissue density mass, which did not rule out local recurrence (left upper panel, arrow). The PET/CT image shows abnormal FDG uptake (SUV_{max}, 4.73) corresponding to this mass, suggesting local recurrence (left lower panel, arrow). A follow-up PET/CE-CT image, which was performed 3 months after the initial examination, revealed an increase in the size and FDG uptake (SUV_{max}, 6.99) of the mass (right panel, arrow), indicating that the initial diagnosis of local recurrence by PET/CE-CT was correct.

the N factor, which is consistent with previous reports.[16,17] On the other hand, PET/CE-CT is very useful in evaluation of the M factor, as indicated by the high accuracy rate of PET/CE-CT within this context. In fact, the diagnostic accuracy rate of PET/CE-CT for the M factor was 94% in 31 patients with stage IVa resectable cancers. Furthermore, in 65 patients with stage IVb

unresectable cancers, the detection rates of PET/CE-CT for metastases to the lymph nodes (N3), liver, peritoneum, lung, and bone were 51%, 55%, 53%, 18%, and 24%, respectively. These detection rates for distant lymph node (N3) and peritoneum metastases were significantly higher for PET/CE-CT imaging than for abdominal CE-CT imaging. The detection rates of PET/CE-CT for lung and bone metastases were also higher than those of abdominal CE-CT imaging. However, such differences were attributed to the nature of PET/CE-CT scans (whole body imaging) and abdominal CE-CT scans (imaging of only a segmental area). Therefore, in the preoperative evaluation of the extent of pancreatic cancer, which is important for deciding treatment options, our present results suggest that PET/CE-CT is a useful tool for assessing T and M factors but is not very useful for assessing the N factor. This is consistent with a report by Strobel et al,[18] in which PET/CE-CT was found to be superior to PET imaging alone in assessing the respectability of pancreatic cancer.

When PET was first developed, many published reports stated that the SUV_{max} could be useful for differentially diagnosing malignancies and benignancies.[16,19] Nishiyama et al[20] and Nakamoto et al[21] reported that a malignancy could be differentiated from a benignancy in pancreatic disorders based on the SUV_{max}-to-delayed scan ratio. However, as described in the present study, the SUV_{max} of malignant pancreatic tumors overlapped with that of benign pancreatic diseases, suggesting that distinguishing between benign and malignant cases through SUV_{max}-based diagnosis is difficult. Extremely high SUV_{max} values were observed in 2 cases of benign pancreatic endocrine tumor in the present study. The SUV_{max} varies according to the several factors, including blood glucose levels, Glut 1 expression, glucose-6-phosphatase expression, and tumor heterogeneity, and others.[16] In a previous study, high SUV_{max} values were found in tumors with high Glut 1 expression.[22] In our study, extremely high SUV_{max} values were observed in 2 cases of benign endocrine tumors, and these high values may be attributed to high Glut 1 expression in these tumors; however, Glut 1 expression was not examined histologically. To differentiate between benignancy and malignancy of pancreatic tumor lesions by PET/CE-CT imaging, we first assessed the invasion of the tumors into surrounding organs/vessels and other malignancy—indicating signs by analysis of the CE-CT portion of PET/CE-CT imaging and then diagnosed the case by referring to the FDG uptake data (SUV_{max}) by analysis of the PET portion. We did not use SUV_{max} values for differentiating between benignancy and malignancy. So, what is the meaning of SUV_{max} in the clinical management of pancreatic cancer? In the present study, we examined correlations between the SUV_{max}, Ts, and tumor marker (CA 19-9) levels in unresectable locally advanced pancreatic cancer under treatment. During the course of treatment, SUV_{max} and CA 19-9 levels showed substantial positive correlations in the change rate, whereas SUV_{max} and Ts showed significant, although slight, positive correlations. However, no significant correlation was found between tumor marker levels and Ts. Treatment effects on solid tumors were assessed by determining Ts by imaging according to the RECIST criteria[12] and by the levels of serum tumor markers. In pancreatic cancer, however, changes in Ts do not necessarily reflect treatment effects because pancreatic cancers contain a variety of interstitial components. Thus, we have frequently experienced discrepancies between changes in Ts and tumor marker levels in assessing the effects of treatment, which makes it difficult to determine the effects of treatment in these cases. Identification of an additional indicator would help in determining the effects of treatment on pancreatic cancer progression/regression. In the present study, we demonstrated that the SUV_{max} measured by PET proved useful in this regard. Similarly, Yoshioka et al[23] reported that the SUV_{max} was useful to monitor the effects of treatment on pancreatic cancers. These findings, together with those in the present study, suggest that the SUV_{max} is a useful indicator for the effects of treatment on pancreatic cancer. The addition of the SUV_{max} to the existing indicators (Ts and markers) is expected to reduce the difficulty of assessing the effects of treatment on pancreatic cancer progression.

Because either invasion into the surrounding regions or distant metastasis is often already involved at the time of pancreatic cancer diagnosis, less than 20% of cases are treated surgically.[24] Even when surgery is used, recurrence usually occurs very soon thereafter.[13] Therefore, cautious observation is required after surgery. In general, abdominal CE-CT is conducted every 3 to 6 months for postoperative monitoring. Local, hepatic, and peritoneal recurrences are frequently observed postoperatively. Abdominal CE-CT can be used to diagnose hepatic recurrence, but it is sometimes difficult to detect local or peritoneal recurrences because of postoperative changes in the anatomical positions of organs.[15,17] Ruf et al[25] showed that FDG-PET is superior to CT/magnetic resonance imaging in the detection of local recurrences of pancreatic cancers. In the present study, we demonstrated that the diagnostic accuracy of PET/CE-CT is superior to abdominal CE-CT in predicting the postoperative local recurrence of pancreatic cancer. Considering the postoperative changes in the anatomical positions of abdominal organs, PET/CE-CT imaging, which uses both CE-CT and PET functions, is recommended for postoperative monitoring.

CONCLUSIONS

In the present study, we demonstrated that PET/CE-CT imaging can provide useful information in the clinical management of pancreatic cancer. We recommend PET/CE-CT imaging as the first choice examination for suspected pancreatic cancer, staging, assessment of treatment effectiveness, and confirmation of suspected recurrence.

REFERENCES

1. Jemal A, Siegel R, Xu J, et al. Cancer statistics, 2010. *CA Cancer J Clin*. 2010;60:277–300.
2. Matsuda T, Marugame T, Kamo K, et al. Cancer incidence and incidence rates in Japan in 2003: based on data from 13 population-based cancer registries in the Monitoring of Cancer Incidence in Japan (MCIJ) Project. *Jpn J Clin Oncol*. 2009;39:850–858.
3. Burris HA 3rd, Moore MJ, Andersen J, et al. Improvements in survival and clinical benefit with gemcitabine as first-line therapy for patients with advanced pancreas cancer: a randomized trial. *J Clin Oncol*. 1997;15:2403–2413.
4. Okusaka T, Funakoshi A, Furuse J, et al. A late phase II study of S-1 for metastatic pancreatic cancer. *Cancer Chemother Pharmacol*. 2008;61:615–621.
5. Smith SL, Rajan PS. Imaging of pancreatic adenocarcinoma with emphasis on multidetector CT. *Clin Radiol*. 2004;59:26–38.
6. Ell PJ. The contribution of PET/CT to improved patient management. *Br J Radiol*. 2006;79:32–36.
7. Reinartz P, Wieres FJ, Schneider W, et al. Side-by-side reading of PET and CT scans in oncology: which patients might profit from integrated PET/CT? *Eur J Nucl Med Mol Imaging*. 2004;31:1456–1461.
8. Isaji S, Kawarada Y, Uemoto S. Classification of pancreatic cancer: comparison of Japanese and UICC classifications. *Pancreas*. 2004;28:231–234.
9. Otsuki M. Chronic pancreatitis in Japan: epidemiology, prognosis, diagnostic criteria, and future problems. *J Gastroenterol*. 2003;38:315–326.

10. Okazaki K, Kawa S, Kamisawa T, et al. Clinical diagnostic criteria of autoimmune pancreatitis: revised proposal. *J Gastroenterol.* 2006;41:626–631.
11. DeLellis R, Lloyd R, Heitz P, et al, eds. *Pathology and Genetics Tumor of Endocrine Organs (World Health Organization Classification of Tumors).* Lyon, France: IARC Press; 2004.
12. Therasse P, Arbuck SG, Eisenhauer EA, et al. New guidelines to evaluate the response to treatment in solid tumors. European Organization for Research and Treatment of Cancer, National Cancer Institute of the United States, National Cancer Institute of Canada. *J Natl Cancer Inst.* 2000;92:205–216.
13. Geer RJ, Brennan MF. Prognostic indicators for survival after resection of pancreatic adenocarcinoma. *Am J Surg.* 1993;165:68–72.
14. Goldberg RM, Fleming TR, Tangen CM, et al. Surgery for recurrent colon cancer: strategies for identifying resectable recurrence and success rates after resection. Eastern Cooperative Oncology Group, the North Central Cancer Treatment Group, and the Southwest Oncology Group. *Ann Intern Med.* 1998;129:27–35.
15. Barkin JS, Goldstein JA. Diagnostic approach to pancreatic cancer. *Gastroenterol Clin North Am.* 1999;28:709–722.
16. Higashi T, Saga T, Nakamoto Y, et al. Diagnosis of pancreatic cancer using fluorine-18 fluorodeoxyglucose positron emission tomography (FDG PET)—usefulness and limitations in "clinical reality." *Ann Nucl Med.* 2003;17:261–279.
17. Zimny M, Bares R, Fass J, et al. Fluorine-18 fluorodeoxyglucose positron emission tomography in the differential diagnosis of pancreatic carcinoma: a report of 106 cases. *Eur J Nucl Med.* 1997;24:678–682.
18. Strobel K, Heinrich S, Bhure U, et al. Contrast-enhanced ^{18}F-FDG PET/CT: 1-stop-shop imaging for assessing the resectability of pancreatic cancer. *J Nucl Med.* 2008;49:1408–1413.
19. Delbeke D, Rose DM, Chapman WC, et al. Optimal interpretation of FDG PET in the diagnosis, staging and management of pancreatic carcinoma. *J Nucl Med.* 1999;40:1784–1791.
20. Nishiyama Y, Yamamoto Y, Monden T, et al. Evaluation of delayed additional FDG PET imaging in patients with pancreatic tumour. *Nucl Med Commun.* 2005;26:895–901.
21. Nakamoto Y, Higashi T, Sakahara H, et al. Delayed (18)F-fluoro-2-deoxy-D-glucose positron emission tomography scan for differentiation between malignant and benign lesions in the pancreas. *Cancer.* 2000;89:2547–2554.
22. Higashi T, Tamaki N, Honda T, et al. Expression of glucose transporters in human pancreatic tumors compared with increased FDG accumulation in PET study. *J Nucl Med.* 1997;38:1337–1344.
23. Yoshioka M, Sato T, Furuya T, et al. Role of positron emission tomography with 2-deoxy-2-[^{18}F]fluoro-D-glucose in evaluating the effects of arterial infusion chemotherapy and radiotherapy on pancreatic cancer. *J Gastroenterol.* 2004;39:50–55.
24. Wray CJ, Ahmad SA, Matthews JB, et al. Surgery for pancreatic cancer: recent controversies and current practice. *Gastroenterology.* 2005;128: 1626–1641.
25. Ruf J, Lopez Hanninen E, Oettle H, et al. Detection of recurrent pancreatic cancer: comparison of FDG-PET with CT/MRI. *Pancreatology.* 2005;5:266–272.

The bisphosphonate incadronate inhibits intraperitoneal dissemination in an *in vivo* pancreatic cancer model

SOICHI TAKIGUCHI[1], YUKIKO NISHINO[1], KAZUKO INOUE[1], MIYAKO IKEDA[3], YASUFUMI KATAOKA[3], KIMIHIKO MATSUSUE[4], KENICHI NISHIYAMA[2] and HARUO IGUCHI[5]

[1]Institute for Clinical Research and [2]Department of Pathology, National Kyushu Cancer Center, Fukuoka 811-1395; Departments of [3]Pharmaceutical Care and Health Sciences and [4]Hygiene Chemistry, Faculty of Pharmaceutical Sciences, Fukuoka University, Fukuoka 814-0180; [5]Clinical Research Institute, Shikoku Cancer Center, Matsuyama 791-0280, Japan

Received January 17, 2012; Accepted March 14, 2012

DOI: 10.3892/or.2012.1757

Abstract. Pancreatic cancer is characterized by intraperitoneal dissemination and often by large volumes of ascites. Aminobisphosphonates exhibit potent antitumor effects and are currently being tested against human solid tumors. Several aminobisphosphonates inhibit cancer cell migration by preventing the activation of Rho through inhibition of the mevalonate pathway. We evaluated the ability of an aminobisphosphonate, incadronate, to inhibit the growth of disseminated pancreatic cancer *in vivo*. We established an *in vivo* pancreatic cancer model with i.p. carcinomatosis in nude mice. Incadronate administration started from the day of tumor inoculation, and reduced tumor burden and ascites accumulation. Further, we evaluated the effect of incadronate on the inhibition of pancreatic cancer cell proliferation, migration and invasion *in vitro*. Incadronate induced growth inhibition and apoptotic death of pancreatic cancer cells. It also inhibited migration presumably by preventing the activation of Rho by lysophosphatidic acid. Thus, the *in vivo* antitumor effect may result from the inhibition of cancer cell proliferation and migration. The potent effects of incadronate in reducing tumor burden and ascites suggest that it will be of value in regimens for the treatment of pancreatic cancer.

Introduction

Pancreatic cancer is the fourth most common cause of cancer death in men and women in the United States, with a 5-year survival for all stages of the disease of less than 5% (1). Pancreatic cancer has no clear early warning signs or symptoms and is usually silent until the disease is well advanced. During the progression of pancreatic cancer, hepatic metastasis and peritoneal dissemination are frequently seen as a distant metastasis, which results in a short survival period. Patients have a median survival of 4-8 months after diagnosis due to the advanced stage of disease by the time it has been discovered and treatment has begun. The anti-metabolite agent gemcitabine is currently being employed to treat pancreatic cancer (2). While gemcitabine has shown a significant benefit in clinical applications, its ability to impact pancreatic cancer is limited. Therefore, new therapeutic approaches need to be investigated to improve the treatment of this neoplasm (3).

One new therapeutic strategy is to clarify the mechanism of metastasis of cancer cells and to identify agents that prevent cancer cells from invading or migrating into the peritoneum. Among many growth-promoting factors known to be present in pancreatic cancer ascites, lysophosphatidic acid (LPA) is found in significant levels and may play an important role in the development or progression of ovarian (4,5) and pancreatic cancer (6). LPA has been reported to induce many cellular effects, including mitogenesis, the secretion of proteolytic enzymes, and migration activity (7).

Cell migration is regulated by a combination of different processes: the contraction of actomyosin, the formation of stress fibers, and the turnover of focal adhesions (8). Contraction of the actomyosin system is important for cell migration, and LPA induces myosin light-chain phosphorylation through the activation of the small GTP-binding protein (G protein) Rho, leading to the stimulation of cell contractility and motility (9). Another fundamental component affecting cell motility is focal adhesions (cell-extracellular matrix adhesions) (8). Rho is a key mediator in the assembly of structures involved in focal adhesion. Changes in the expression and activities of the components of focal adhesions may contribute to cancer invasion (10). Interfering with the LPA signal transduction pathway by modulating Rho activity may be an attractive strategy for improving the outcome of pancreatic cancer.

Aminobisphosphonates (N-BPs) are potent inhibitors of bone resorption used for the treatment and prevention of osteoporosis. N-BPs have been shown to inhibit the cholesterol biosynthesis pathway as well as isoprenylation (farnesylation and geranylgeranylation) by inhibiting either isopentanyl diphosphate synthase or a downstream enzyme, farnesyl diphosphate synthase, or both (11). Protein targets of isoprenylation include small G proteins

Correspondence to: Dr Haruo Iguchi, Clinical Research Institute, Shikoku Cancer Center, Minamiumemotomachi Ko160, Matsuyama, Ehime 791-0280, Japan
E-mail: higuchi@shikoku-cc.go.jp

Key words: bisphosphonate, apoptosis, pancreatic cancer, intraperitoneal dissemination, Rho

such as Rho, Ras, Rac, and Rab, which require post-translational modification to undergo a series of changes that lead to their attachment to the plasma membrane and their full activation. The activation of small G proteins is essential for cancer cell growth and invasion (12,13). Accordingly, N-BPs have the potential to inactivate the small G proteins that regulate cancer cell growth, motility, and invasion (14,15). Treatment of ovarian cancer cells with alendronate, an N-BP, resulted in the inactivation of Rho, changes in cell morphology, loss of stress fiber formation, and focal adhesion assembly (16). Furthermore alendronate markedly inhibited the invasiveness of human ovarian cancer cells in a model of i.p. ovarian carcinomatosis (17).

In the present study, we evaluated the ability of incadronate (INC), an N-BP, to inhibit the growth of disseminated pancreatic cancer *in vivo*. We established an *in vivo* pancreatic cancer model with i.p. carcinomatosis in nude mice. INC administration started from the day of tumor inoculation, and reduced tumor burden and ascites accumulation. Additionally, we evaluated the effect of INC on the inhibition of pancreatic cancer cell proliferation, migration, and invasion *in vitro*.

Materials and methods

Cell culture. SUIT-2, AsPC-1, and BxPC-3 cell lines were derived from a human pancreatic ductal adenocarcinoma (PDAC). They were cultured in a RPMI-1640 medium (Invitrogen, Carlsbad, CA, USA) supplemented with 5% fetal bovine serum (FBS) and 50 U/ml penicillin and 50 μg/ml streptomycin in a humidified atmosphere under 5% CO_2 at 37°C.

In vitro cell proliferation assay. Cell proliferation was measured using an MTT dye reduction method (18). Briefly, human PDAC cell lines were seeded into 96-well plates ($5x10^3$ cells/100 μl) and allowed to attach for 24 h. Cells were treated with various concentrations of INC (Astellas Pharma, Tokyo, Japan) for 48 h in 100 μl culture medium. At the end of drug exposure, 5 μl MTT stock solution (5 mg/ml PBS) was added to each well, and the cells were further incubated for 4 h at 37°C. Then, 100 μl of DMSO was added to dissolve the dark blue crystals. Absorbance was measured with an MPR-A4 microplate reader (Tosoh, Tokyo, Japan) at test and reference wavelengths of 540 and 620 nm, respectively.

Analysis of apoptosis. SUIT-2 cells were cultured in slide chambers to no more than 50-60% confluence and treated with various concentrations of INC, as described in *in vitro* cell proliferation assay. After 48-h treatment, apoptosis was assessed using an *in situ* cell death detection kit (Roche Applied Science, Mannheim, Germany), following the manufacturer's recommendations. Briefly, cells were washed with PBS once, fixed with 4% buffered paraformaldehyde for 1 h, washed again with PBS, and permeabilized on ice with 0.1% Triton X-100 in 0.1% sodium citrate for 2 min. Slides were rinsed twice with PBS and then incubated for 60 min at 37°C with terminal deoxynucleotidyl transferase enzyme in reaction buffer. The slides were rinsed three times with PBS and mounted with PermaFluor (Thermo Fisher Scientific, Waltham, MA, USA). Samples were analyzed by fluorescence microscopy. TUNEL-positive nuclei were detected by a bright color in condensed or ruptured nuclei. The rate of apoptosis was calculated as the ratio of the number of apoptotic cells to the total number of cells (both apoptotic and non-apoptotic cells).

Cell migration and invasion assays. Transwell cell migration and invasion were evaluated using a 24-well chemotaxis chamber with a membrane of 8 μm pore size (BD Biosciences, Franklin Lakes, NJ, USA). For migration and invasion assays, SUIT-2 cells were incubated in serum-free culture medium with the various concentrations of INC for 24 h and transferred to the upper chamber ($2.5x10^5$ cells/500 μl) with the various concentrations of INC and allowed to migrate through control (non-coated) and Matrigel-coated (8.7 mg/ml) membranes for 24 h, respectively. The lower chambers were filled with culture medium containing 5% FBS with the various concentrations of INC. Non-migrated cells were wiped off with a cotton swab, the filter was stained with Diff-Quik stain solution (Siemens, Munch, Germany), and the number of remaining cells was counted under the microscope. To determine the percent of invasion, the mean number of cells invading through the Matrigel-coated insert membrane was divided by the mean number of cells migrating through the control insert membrane and multiplied by 100.

Rho pull-down assay. The Rho pull-down assay was performed using a Rho activation assay kit according to the manufacturer's instructions (Cytoskeleton, Denver, CO, USA). Briefly, cells ($3x10^5$/ml) were cultured under serum-free conditions with or without various agents for 24 h. After incubation, the cells were stimulated with 2.2 μM LPA for 1 min and lysed in Mg^{2+} lysis buffer. Equal volumes of cell lysates were incubated with Rhotekin-RBD beads. Bound Rho proteins were detected by Western blotting using a monoclonal antibody against RhoA. Western blotting of the total amount of Rho in cell lysates was performed for comparison with Rho activity (level of GTP-bound Rho) in the same samples.

In vivo peritoneal dissemination model of pancreatic cancer. Five-week-old male nude mice (BALB-cAJcl-nu/nu, Clea Japan, Tokyo, Japan) were housed in filtered-air laminar-flow cabinets and were manipulated using aseptic procedures. Procedures involving animals and their care were conducted in conformity with the guidelines of the National Kyushu Cancer Center. To prepare the *in vivo* peritoneal dissemination model, SUIT-2 cells were injected i.p. as a cell suspension into nude mice ($1x10^6$ cells in 200 μl PBS per animal). This model using SUIT-2 is not only simple and reproducible, but also has characteristics that resemble those of human pancreatic cancer. The treatment regimens started on the day of tumor inoculation and continued for 4 weeks. INC was delivered using a PBS vehicle and was administered i.p. every day. The daily doses of INC used were as follows: 0, 0.1, 1, 2, and 3 mg/kg/d. At the end of the treatment period, mice were sacrificed. The volume of ascites was measured, and tumor tissue was excised, weighed, fixed in 10% neutral buffered formalin, and embedded in paraffin. Paraffin sections (5 μm) were used for histological analysis. Sections were stained with hematoxylin and eosin, examined, and photographed under a microscope. Blood samples were collected from the left heart ventricle and assayed for serum CA19-9.

Statistical analysis. Results are reported as the average ± SEM. Group comparisons were performed using a one-way analysis

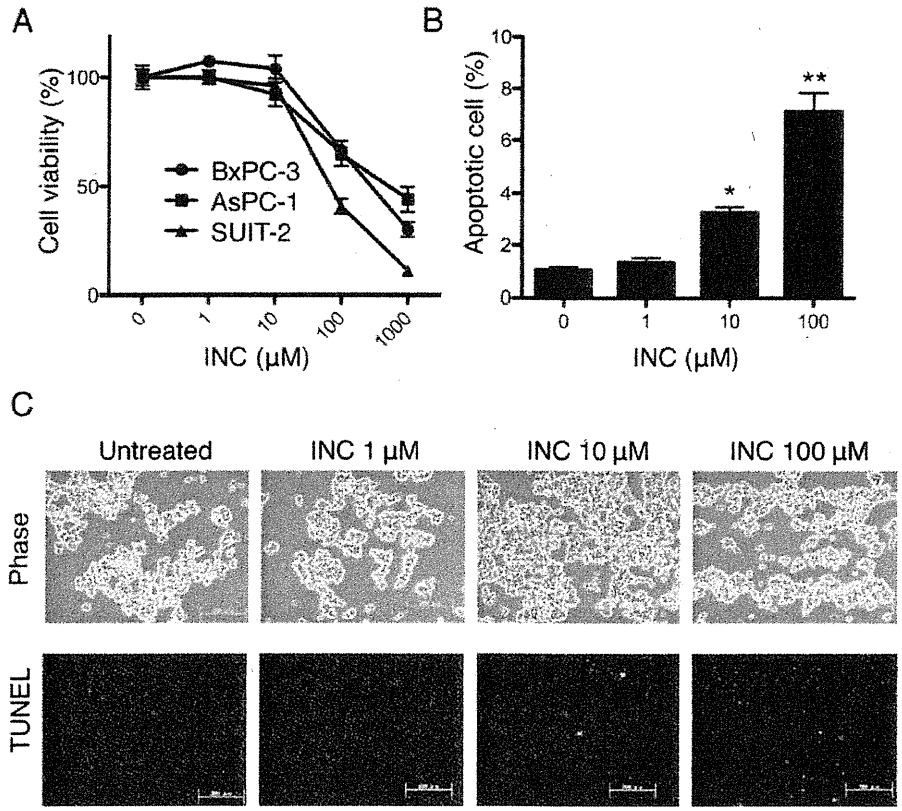

Figure 1. INC induces antiproliferative effects and apoptosis in human PDAC cell lines. (A) BxPC-3, AsPC-1, and SUIT-2 were treated with INC for 48 h. Cell growth inhibition was expressed as a percentage of the absorbance of control cultures measured at 540 nm with a microplate reader. N=6 for each experiment. (B) The rate of apoptosis in SUIT-2 cells treated with INC for 48 h was calculated as the ratio of the number of apoptotic cells to the total number of cells. N=3 for each experiment. *p<0.05, **p<0.01 vs. untreated cells. (C) Representative microscopic photos of SUIT-2 cells treated with INC for 48 h. Phase-contrast microscopy (upper panels) and fluorescent microscopy of TUNEL staining (white) showing apoptotic cells (lower panel). Bar, 200 μm.

of variance (ANOVA) followed by the Tukey-Kramer multiple comparison test. Differences were considered significant at $P<0.05$.

Results

INC induces antiproliferative effects and apoptosis in human PDAC cell lines. The effect of INC on BxPC-3, AsPC-1, and SUIT-2 PDAC cell lines was investigated *in vitro* using the MTT assay. Treatment with INC (1-1000 μM) produced a dose-dependent reduction in cell growth after 48 h of treatment (Fig. 1A) and the IC_{50} was calculated in a range of 50-500 μM. To clarify the mechanisms of INC-induced growth inhibition, we performed a TUNEL assay on SUIT-2 cells, which were the most sensitive to this compound among the three PDAC cell lines tested. Thereafter, we used SUIT-2 cells exclusively in the other experiments. Upon 48-h exposure to INC, the occurrence of apoptosis in 10 and 100 μM INC-treated cells was 3.3 and 7.1% respectively, and was significantly higher than that in untreated cells (1.1%) (Fig. 1B). SUIT-2 cells presented typical apoptotic morphology with cell shrinkage, nuclear condensation and fragmentation, and cellular rupture into debris (Fig. 1C).

Effect of INC on migration and invasion of SUIT-2 in culture. INC was unable to perturb cellular migration toward 5% FBS in chemotaxis chambers at 1 μM (Fig. 2A). At 10 and 100 μM, the inhibition was 49 and 73%, respectively. INC was also potent in its action against the invasion of cells through Matrigel with a 71% inhibition occurring at 10 μM and a 90% inhibition at 100 μM (Fig. 2B). These results are not due to cell cytotoxicity because the degree of cell death after 48-h treatment with INC did not exceed 5 and 10% at 10 and 100 μM INC, respectively. The percent of invasion was 9.6, 10, 5.5, and 3.7% at 0, 1, 10, and 100 μM, respectively (Fig. 2C). Collectively, INC inhibited both migration and invasion of SUIT-2 at a concentration between 10 and 100 μM.

The activation of Rho by LPA is suppressed by INC, and restored by the addition of GGOH in SUIT-2. It is now well established that cell migration is induced by Ras-related GTPases (especially Rho). Soluble factors from serum, such as lysophosphatidic acid (LPA), are thought to activate Rho based on their ability to induce actin stress fibers and focal adhesions in a Rho-dependent manner (19). To evaluate whether LPA induces Rho activity in SUIT-2 cells, we used a pull-down assay with the fusion protein GST- Rhotekin-RBD, which recognizes only Rho-GTP, the active form of Rho. An increase in Rho-GTP was observed in SUIT-2 cells treated for 1 min with LPA (2.2 μM). The inhibitory effect of INC (30 μM) and abrogation by the addition of GGOH (30 μM) suggests INC may inhibit cancer cell migration through Rho geranylgeranylation (Fig. 3).

Effects of INC in a SUIT-2 peritoneal dissemination model. To assess the effect of INC on intraperitoneal dissemination *in vivo*,